

AD\_\_\_\_\_

AWARD NUMBER: DAMD17-02-1-0595

TITLE: Do Perturbed Epithelial-Mesenchymal Interactions Drive Early Stages of Carcinogenesis

PRINCIPAL INVESTIGATOR: Carlos Sonnenschein, M.D.

CONTRACTING ORGANIZATION: Tufts University  
Boston, Massachusetts 02111

REPORT DATE: April 2006

TYPE OF REPORT: Final

PREPARED FOR: U.S. Army Medical Research and Materiel Command  
Fort Detrick, Maryland 21702-5012

DISTRIBUTION STATEMENT: Approved for Public Release;  
Distribution Unlimited

The views, opinions and/or findings contained in this report are those of the author(s) and should not be construed as an official Department of the Army position, policy or decision unless so designated by other documentation.

# REPORT DOCUMENTATION PAGE

*Form Approved*  
*OMB No. 0704-0188*

Public reporting burden for this collection of information is estimated to average 1 hour per response, including the time for reviewing instructions, searching existing data sources, gathering and maintaining the data needed, and completing and reviewing this collection of information. Send comments regarding this burden estimate or any other aspect of this collection of information, including suggestions for reducing this burden to Department of Defense, Washington Headquarters Services, Directorate for Information Operations and Reports (0704-0188), 1215 Jefferson Davis Highway, Suite 1204, Arlington, VA 22202-4302. Respondents should be aware that notwithstanding any other provision of law, no person shall be subject to any penalty for failing to comply with a collection of information if it does not display a currently valid OMB control number. **PLEASE DO NOT RETURN YOUR FORM TO THE ABOVE ADDRESS.**

<b>1. REPORT DATE (DD-MM-YYYY)</b> 01-04-2006		<b>2. REPORT TYPE</b> Final		<b>3. DATES COVERED (From - To)</b> 1 April 2002 – 31 Mar 2006	
<b>4. TITLE AND SUBTITLE</b>  Do Perturbed Epithelial-Mesenchymal Interactions Drive Early Stages of Carcinogenesis				<b>5a. CONTRACT NUMBER</b>	
				<b>5b. GRANT NUMBER</b> DAMD17-02-1-0595	
				<b>5c. PROGRAM ELEMENT NUMBER</b>	
<b>6. AUTHOR(S)</b>  Carlos Sonnenschein, M.D.  E-Mail: <a href="mailto:carlos.sonnenschein@tufts.edu">carlos.sonnenschein@tufts.edu</a>				<b>5d. PROJECT NUMBER</b>	
				<b>5e. TASK NUMBER</b>	
				<b>5f. WORK UNIT NUMBER</b>	
<b>7. PERFORMING ORGANIZATION NAME(S) AND ADDRESS(ES)</b>  Tufts University Boston, Massachusetts 02111				<b>8. PERFORMING ORGANIZATION REPORT NUMBER</b>	
<b>9. SPONSORING / MONITORING AGENCY NAME(S) AND ADDRESS(ES)</b> U.S. Army Medical Research and Materiel Command Fort Detrick, Maryland 21702-5012				<b>10. SPONSOR/MONITOR'S ACRONYM(S)</b>	
				<b>11. SPONSOR/MONITOR'S REPORT NUMBER(S)</b>	
<b>12. DISTRIBUTION / AVAILABILITY STATEMENT</b> Approved for Public Release; Distribution Unlimited					
<b>13. SUPPLEMENTARY NOTES</b>					
<b>14. ABSTRACT</b>  This research project had three specific aims. The first was to determine which tissue in the rat mammary gland was the target of the chemical carcinogen N-nitrosomethylurea. This aim was fulfilled. The second aim included screening and counting lesions and performing morphometric data analysis of whole mounts (branching pattern, relative abundance of the different ductal and alveolar structures). These studies aimed at identifying the changes occurring between the time of exposure and the appearance of neoplasias. This aim was also fulfilled. Finally, as described for Aim #3, during years two and three we explored the specific roles of hyaluronan and emmprin, two molecules that are enriched in tumors and involved in tumor-stromal cell interactions as mediators of neoplastic initiation and progression.					
<b>15. SUBJECT TERMS</b> Carcinogenesis, Tissue Transplants, Nitrosomethylurea, Pathology, Immunohistochemistry, EMPRIN					
<b>16. SECURITY CLASSIFICATION OF:</b>			<b>17. LIMITATION OF ABSTRACT</b>	<b>18. NUMBER OF PAGES</b>	<b>19a. NAME OF RESPONSIBLE PERSON</b>
<b>a. REPORT</b>	<b>b. ABSTRACT</b>	<b>c. THIS PAGE</b>			USAMRMC
U	U	U	UU	41	<b>19b. TELEPHONE NUMBER (include area code)</b>

## Table of Contents

<b>Cover.....</b>	<b>1</b>
<b>SF 298.....</b>	<b>2</b>
<b>Introduction.....</b>	<b>4</b>
<b>Body.....</b>	<b>4</b>
<b>Key Research Accomplishments.....</b>	<b>6</b>
<b>Reportable Outcomes.....</b>	<b>6</b>
<b>Conclusions.....</b>	<b>6</b>
<b>References.....</b>	<b>7</b>
<b>Appendices.....</b>	<b>7</b>

## INTRODUCTION:

The DOD Award Number DAMD17-02-1-0595 research project had three specific aims. As mentioned in the report for year 2, the first aim was to determine which tissue in the rat mammary gland was the target of the chemical carcinogen N-nitrosomethylurea. This aim was fulfilled. The second aim included screening and counting lesions and performing morphometric data analysis of whole mounts (branching pattern, relative abundance of the different ductal and alveolar structures). These studies were directed at identifying the changes occurring between the time of exposure and the appearance of neoplasias. This aim was also fulfilled. Finally, as described for Aim #3, during years two and three we explored the specific roles of hyaluronan and EMMPRIN, two molecules that are enriched in tumors and involved in tumor-stromal cell interactions as mediators of neoplastic initiation and progression.

## BODY:

**HYPOTHESIS:** Are the targets of the carcinogen the genomic DNA of epithelial cells, the stroma, or both? The answer to this question was the stroma. During the three-year period of support we have accomplished the following:

**Aim #1.** The data collected were published (The stroma as a crucial target of chemical carcinogens in the rat mammary gland. Maricel V. Maffini, Ana M. Soto, Janine M. Calabro, Angelo A. Ucci and Carlos Sonnenschein, *Journal of Cell Science*, 117, 1495-1502, 2004). This publication merited being editorialized in the same issue of the *Journal of Cell Science* (**Weaver VM, Gilbert P** 2004 Watch thy neighbor: cancer is a communal affair. *Journal of Cell Science* 117:1495-1502)

Briefly, only those animals whose stroma was exposed to NMU developed neoplasias, regardless of whether or not the transplanted mammary epithelial cells were exposed to the carcinogen. The Ha-ras mutation was also assessed in DNA isolated from NMU-exposed and non-exposed mammary epithelial cells, mammary fibroblasts, and mammary pre-adipocytes collected from intact virgin rats and grown *in culture*. The presence of the mutation did not correlate with cell type, culture conditions or carcinogen treatment. These results highlighted the need to explore the roles that the stroma components play in rodent mammary carcinogenesis; these components include the cells (fibroblasts, adipocytes, macrophages, mast cells) and the extracellular matrix. The next step will be to explore the role of the stroma in 3-dimensional tissue culture models for carcinogenesis. We have identified novel silkworm fibroins that form scaffoldings and mats as a promising experimental model where cellular and extracellular components of the mammary gland will be studied.

**Aim #2.** To establish a pattern of the dynamic, temporal response of the stroma and the epithelium of the different combinations of tissue involved in mammary carcinogenesis as outlined in **Aim #1**. Our experimental results and those by other groups indicated that the mammary glands are most vulnerable to chemical carcinogenesis at puberty and become resistant as the rats age. Maximal resistance is achieved after pregnancy and lactation. In the same context of Aim #1, we explored the role of the stroma during what we interpreted as tumor inhibition. Namely, we assessed whether the ability of the cleared mammary gland fat pad (CFP) to normalize cancer cells varied during diverse physiological states, more specifically, the age of the host. A pilot study revealed that epithelial carcinoma cells (ECCs) formed tumors when injected in CFPs of “young” (24 and 50 day-old) hosts. In contrast, tumor development was substantially inhibited or absent when tumor cells were injected into CFP of “adult” (80 and 150 day-old) or multiparous hosts (after 2 pregnancies followed by complete nursing of pups). Most remarkably, these data suggested a parallel to the phenomenon of age-dependent susceptibility and resistance to chemical carcinogens. That is, the incidence of transplanted tumors decreased as the age at which rats were inoculated with tumor cells increased. In addition, twice-pregnant rats developed no tumors from the tumor cells implanted (see Figure 1, below). This experiment was completed

during the third year of funding and has now been published in the American Journal of Pathology (Maffini, Calabro et al. 2005).

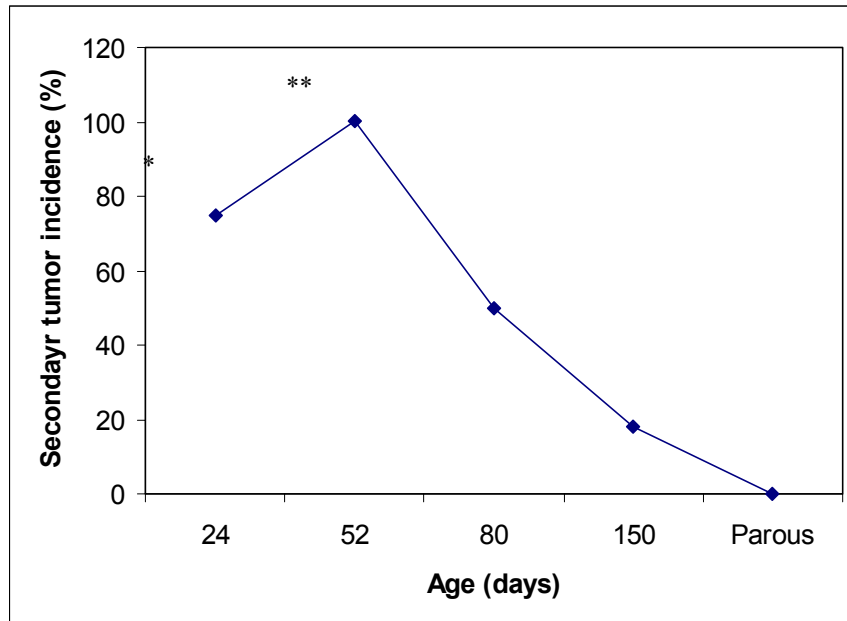
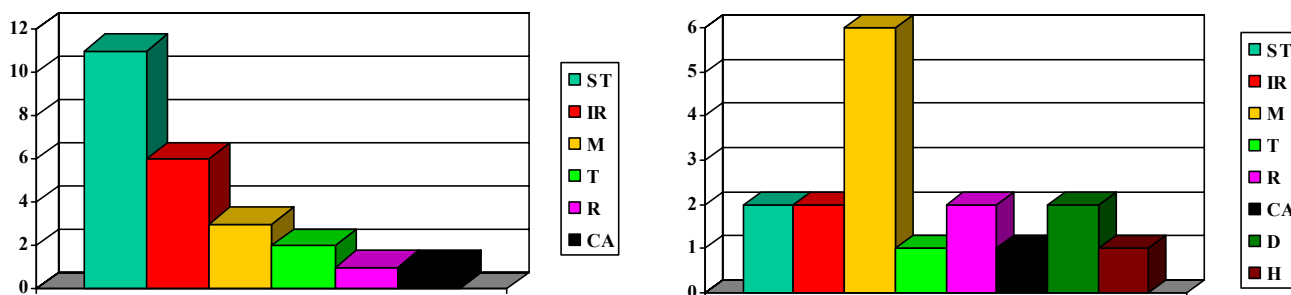


Fig.1: The incidence of secondary tumors decreased with the age of the stroma. The parous host only developed normal ductal outgrowths. \*\*Statistically different from twice-parous, 150- and 80-day-old host groups. \* Statistically different from twice-parous, and 150-day-old host groups.

Hence, susceptibility to chemical carcinogens and the ability to reprogram the neoplastic behavior seem to be linked to aging; more specifically, the ability of these tumors cells to organize as ducts or as tumors is regulated by the age of the stroma in which they are implanted. Thus, as susceptibility to carcinogenesis decreases, the ability of the stroma to reprogram neoplastic epithelial cells as normal epithelial duct cells increases. This observation strongly supports the notion that the neoplastic phenotype is context-dependent and, hence, it offers the intriguing possibility that the process of carcinogenesis is amenable to normalization or “cure” once the mechanisms of stroma-mediated “normalization” are elucidated.

**Aim #3.** To define the relationship between early carcinogenic events and peri- and extracellular markers that are known to affect the proliferative and invasive behavior of cancer cells. We tried to optimize the protocols to characterize EMMPRIN and hyaluronic acid expression using immunohistochemistry and histochemistry techniques, respectively. EMMPRIN was localized in the epithelial cells while HA was mostly localized in the fibroblasts of the periductal stroma. Both histochemical reactions showed a very high background with spurious staining of the fat pad. Despite redoubled efforts to resolve this technical problem, it could not be circumvented. Quantification of hyaluronic acid using an ELISA assay could not be performed due to technical problems. In addition to these technical problems, the earliest evidence for ductal structures in recombined mammary glands occurred not before 60 days following the injection of 50,000 tumor cells. Renewed efforts to refine an ELISA were unsuccessful and this precluded observing hyaluronic acid and EMMPRIN expression during early neoplastic development. The alternative to further pursue this line of investigation would have made us incur into expenditures of animals and culture components beyond the budget allotted to these activities by the DOD. To remedy this situation, we opted to gain information about early events in rat mammary gland carcinogenesis by performing DNA microarrays. Genome-wide DNA Microarray analysis was performed with RNA extracted from the cleared mammary fat pads of rats treated with vehicle or 50 mg/kg NMU at 50 days of age. The mammary glands were harvested 5 days later (the time of recombination with epithelial cells). To avoid confounding by hormonal status, only animals in proestrus were used. We found that NMU treatment resulted

in 37 genes being up-regulated genes (17 were EST) and 36 genes being down-regulated (19 were EST) at a ratio of 1.5 ( $p=0.05$ ). Ontology analysis resulted in the following categories being significantly up-regulated: IR: immune response (6 genes), ST: signal transduction (11 genes), M: metabolism (3 genes), CA: cell adhesion (1 gene), R: receptor (1 gene) and T: transcription (2 genes). We are completing the analysis of these data and preparing a manuscript for publication.



**Frequency of gene expression in mammary gland stroma:** The graph on the left represents the ontology of the up-regulated genes and the graph on the right represents the down-regulated genes. The data represents the genes that were expressed higher than 1.5 fold and have a  $p$  value higher than 0.05

To accommodate a novel perspective on the role of the stroma in carcinogenesis, a rigorous analysis of concepts, definitions and experimental approaches is now needed. This will facilitate the identification of the mediators responsible for the altered tissue phenotype in cancers and of ways to reverse their effect by adopting a solid epigenetic perspective.

## KEY RESEARCH ACCOMPLISHMENTS:

- We have completed **Aim 1**: the results clearly establish that the stroma is a main target of chemical carcinogens and suggest that carcinogenesis is a tissue organization-based problem.
- Our data collected while developing **Aim 2** strengthened the notion that the stroma is the most prominent target of the carcinogen and, equally important, the stroma has the capacity to “normalize” the neoplastic properties of rat mammary gland tumors.
- The histochemical techniques needed to explore the original **Aim # 3** could not be optimized because of technical problems. Instead, we explored the early carcinogenic events by using DNA microarrays in order to define which genes and groups of genes are differentially expressed during these early stages of carcinogenesis. We are currently processing these data to be included in a publication that is now in preparation.

## REPORTABLE OUTCOMES:

- Preliminary data was presented in the 12<sup>th</sup> International Conference of the International Society of Differentiation. (see enclosed abstract)
- A paper was published reporting the results of **Aim # 1** (see enclosed JCS paper).
- A paper was published reporting the results of **Aim # 2** (see enclosed AJP paper).
- Presentations of our observations were made at the 2002 and 2003 Gordon Research Conferences, the 2005 Keystone Conferences and 2005 DOD Era of Hope meetings.

## CONCLUSIONS:

Under a theory-neutral experimental design, we tested whether the primary target of the carcinogen was the epithelium, the stroma, or both tissue compartments. We concluded that neoplastic transformation of mammary epithelial cells occurred only when the stroma was exposed *in vivo* to N-nitrosomethylurea, regardless of whether or not the epithelial cells were exposed to the carcinogen. Mutation in the Ha-ras-1 gene did not correlate with initiation of neoplasia. Thus, our results suggest that the stroma is a crucial target of the carcinogen and that mutation in the Ha-ras-1 gene is neither necessary nor sufficient for tumor initiation. Next, we have found evidence that the ability of the stroma to induce and to curtail neoplastic behavior is age-dependent. That is, rat epithelial mammary tumor cells injected in cleared fat pads of isogenic hosts developed following a pattern comparable to that followed when the carcinogen NMU is injected to rats of different ages and also to rats that have gone through two pregnancies. In other words, the stroma of the host rats is affected by age and by pregnancy; as a result, either cellular or extracellular components, or both, are able to modulate the ability of tumor cells in their ability to either grow as tumors or to form a phenotypically normal ductal tree. These observations merit a closer look at the interactions among these tumor cells and stromal cells and extracellular molecules.

## **REFERENCES:**

Soto AM, Maffini MV, Calabro JM, Wieloch C, Sonnenschein C: Mammary gland stroma is responsible for epithelial cell neoplasia. *Differentiation* 70:321, 2002

Maffini MV, Soto AM, Calabro JM, Ucci AA, and Sonnenschein C: The stroma as a crucial target of chemical carcinogens in the rat mammary gland. *Journal of Cell Science*, 117, 1495-1502, 2004.

Maffini MV, Calabro JM, Soto AM, Sonnenschein C: Stromal regulation of neoplastic development: Age-dependent normalization of neoplastic mammary cells by mammary stroma. *American Journal of Pathology* 2005; 67: 1405-10

Soto AM, Sonnenschein C: Emergentism as a default: cancer as a problem of tissue organization. *Journal of Biosciences* 2005; 30: 103-18

Soto AM, Sonnenschein C: The somatic mutation theory of cancer: growing problems with the paradigm? *BioEssays* 2004; 26: 1097-107

Sonnenschein C, Soto AM: Are times a' changin' in carcinogenesis? *Endocrinology* 2005; 146: 11-2

Sonnenschein C, Soto AM: Carcinogenesis and metastasis now in the third dimension- What's in it for pathologists? *American Journal of Pathology* 2006; 168: 363-6

## **APPENDICES:**

Soto AM, Maffini MV, Calabro JM, Wieloch C, Sonnenschein C: Mammary gland stroma is responsible for epithelial cell neoplasia. *Differentiation* 70:321, 2002

Maffini MV, Soto AM, Calabro JM, Ucci AA and Sonnenschein C: The stroma as a crucial target of chemical carcinogens in the rat mammary gland. *Journal of Cell Science*, 117, 1495-1502, 2004

Maffini MV, Calabro JM, Soto AM, Sonnenschein C: Stromal regulation of neoplastic development: Age-dependent normalization of neoplastic mammary cells by mammary stroma. *American Journal of Pathology* 2005; 67: 1405-10



dence that a distinct TA cell population can be reprogrammed and that they do so by first reverting to hair stem cells.

**S4-ST2: Mammary gland stroma is responsible for epithelial cell neoplasia**

Soto AM\*, Maffini MV, Calabro JM, Wieloch C, Sonnenschein C  
Tufts University School of Medicine, 136 Harrison Ave.  
Boston, MA 02111, USA

Mammary gland development is driven by a network of signals between stroma and epithelium. The tissue organization field theory of carcinogenesis (TOFT) proposes that altered reciprocal interactions between stroma and epithelium initiate the neoplastic process. We assessed whether the primary target of the carcinogen N-nitroso-methylurea (NMU) in mammary glands of Wistar-Furth rats is the epithelium, the stroma, or both. The 4th and 5th mammary gland fat pads were cleared of epithelium (CFP) at 21 days of age. One month later, these animals were treated with NMU (Groups 1 and 2) or vehicle (3 and 4). One week later, vehicle-treated epithelial cells were transplanted into the CFP of Groups 1 and 4, while NMU-treated epithelial cells were transplanted into the CFP of Groups 2 and 3. Also, positive and negative controls consisting of intact virgin rats injected respectively with NMU (Group 5), and vehicle (Group 6) were included. Tumors appeared in Group 1 (92.8%), 2 (75%), and 5 (100%) and were absent in Groups 3, 4, and 6. Whole-mount preparations and histology confirmed the mammary tumor origin of the palpable lesions. Our results suggest that only the stroma is the target of the carcinogen. This novel concept in carcinogenesis should provide for a more rational study of breast cancer.

**Posters**

**S4-P1: From ectodermal buds towards epidermal appendages: Does keratin expression play a role in early mammary gland development?**

Al-Dahmash AM\*, Lane EB  
Cancer Research UK Cell Structure Research Group,  
School of Life Sciences, University of Dundee,  
Dundee DD1 4HN, UK

Mammary gland development starts with a group of cells, the mammary bud, invading the underlying mesenchyme as an in-growth from the single-layered ectoderm. To understand and study the molecular events that contribute to the revolution of a bud to become a mammary gland, it is essential to understand the cellular context in which these events are occurring.

Keratin expression is linked to the state of epithelial differentiation and has been shown to be involved in cell,

and subsequently tissue, physical stability. Despite this, little is known about the expression or the role of keratins in mammary gland development. In addition, it is not known if the mesenchyme has any direct influence that leads to changes in the bud cells' keratin expression.

In this study, the expression of keratins, desmosomal, hemidesmosomal, and extracellular matrix proteins have been examined at different stages of embryonic mouse mammary gland development. The results show that there are site-specific expression patterns of some keratins and desmosomal proteins within the bud. In addition, a loss of expression of a number of extracellular matrix proteins and hemidesmosome proteins is observed around the mammary gland.

Loss of cell-cell or cell-substrate adhesion may be needed to reposition cells to form new structures. Alterations in the expression of structural proteins including those which are in the extracellular matrix junctions may change the physical properties of the epithelia making it stiffer, or more plastic as appropriate, which may help determine the way a tissue changes shape.

**S4-P2: Nidogen controls basement membrane assembly in 3D-co-culture**

Breitkreutz D\*<sup>1</sup>, Schmidt C<sup>1</sup>, Stark HJ<sup>1</sup>, Mirancea N<sup>2</sup>, Nischt R<sup>3</sup>, Werner U<sup>4</sup>, Fusenig NE<sup>1</sup>

<sup>1</sup>German Cancer Research Center, Division B0600, Heidelberg, Germany; <sup>2</sup>Rumanian Academy of Sciences, Bucharest, Rumania; <sup>3</sup>Department of Dermatology, University of Cologne, Cologne, Germany; <sup>4</sup>Aventis-Germany, Frankfurt/Main, Germany

Skin physiology can be mimicked in organotypic 3D-co-cultures of keratinocytes and fibroblasts, being herein employed to study basement membrane (BM) formation. The 3D-co-culture consisted of human keratinocytes (HK) growing on type I collagen gels populated by human (HF) or murine fibroblasts (MF). The BM-zone was analyzed at various time points by indirect immunofluorescence (IIF), confocal laser scan microscopy, regular (EM) and immuno-electron microscopy (ImEM). To address mechanisms in BM-assembly, we primarily focused on the role of nidogen (ND). Initially, ND-binding to laminin-10 (LN-10) was inhibited with the recombinant laminin gamma1,III3-5 fragment (Lg1f). In 3D-co-culture, this completely blocked deposition of ND, LN-10, and perlecan at the matrix interface (during 10-21 days), while continuous lining was seen by type IV collagen (CIV). Most components of BM-adhesion complexes, such as LN-5, CXVII, and integrin alpha6beta4, were not, or only mildly, affected by Lg1f, but defined hemidesmosomes were entirely missing (EM, ImEM). Since ND is exclusively synthesized by fibroblasts, we applied MF from ND1/ND2 knockout mice together with HK in 3D-co-cultures. So far, with (-/+ +) MF,

# The stroma as a crucial target in rat mammary gland carcinogenesis

Maricel V. Maffini<sup>1</sup>, Ana M. Soto<sup>1,\*</sup>, Janine M. Calabro<sup>1</sup>, Angelo A. Ucci<sup>2</sup> and Carlos Sonnenschein<sup>1</sup>

<sup>1</sup>Department of Anatomy and Cellular Biology, Tufts University School of Medicine, 136 Harrison Avenue, Boston, MA 02111, USA

<sup>2</sup>Department of Pathology, Tufts-New England Medical Center, 750 Washington Street, Boston, MA 02111, USA

\*Author for correspondence (e-mail: ana.soto@tufts.edu)

Accepted 20 November 2003

Journal of Cell Science 117, 1495-1502 Published by The Company of Biologists 2004  
doi:10.1242/jcs.01000

## Summary

A complex network of interactions between the stroma, the extracellular matrix and the epithelium drives mammary gland development and function. Two main assumptions in chemical carcinogenesis of the mammary gland have been that carcinogens induce neoplasia by causing mutations in the DNA of the epithelial cells and that the alterations of tissue architecture observed in neoplasms are a consequence of this primary mutational event. Here, we use a rat mammary tissue recombination model and the chemical carcinogen *N*-nitrosomethylurea (NMU) to determine whether the primary target of the carcinogen is the epithelium, the stroma or both tissue compartments. Mammary epithelial cells were exposed *in vitro* either to the carcinogen or vehicle before being transplanted into the cleared fat pads of rats exposed to carcinogen or vehicle. We observed that neoplastic transformation of these

mammary epithelial cells occurred only when the stroma was exposed *in vivo* to NMU, regardless of whether or not the epithelial cells were exposed to the carcinogen. Mammary epithelial cells exposed *in vitro* to the carcinogen formed phenotypically normal ducts when injected into a non-treated stroma. Mutation in the *Ha-ras-1* gene did not correlate with initiation of neoplasia. Not only was it often found in both cleared mammary fat pads of vehicle-treated animals and intact mammary glands of untreated animals, but it was also absent in some tumors. Our results suggest that the stroma is a crucial target of the carcinogen and that mutation in the *Ha-ras-1* gene is neither necessary nor sufficient for tumor initiation.

Key words: Mammary carcinogenesis, Stroma, Neoplasms, *N*-nitrosomethylurea, NMU, *Ha-ras-1* mutation, Tissue architecture

## Introduction

A comprehensive understanding of carcinogenesis in general, and in the rat mammary gland in particular, has been delayed because of epistemological issues. It has been obvious to many of us working in the field of carcinogenesis that we lack a consistently reliable set of premises on which we can base a solid rationale to conduct research (Sonnenschein and Soto, 1999a; Sonnenschein and Soto, 2000; Moss, 2003). For almost a century, a majority of researchers have followed the lead provided by Theodor Boveri in 1914, favoring the notion that carcinogenesis occurs at the cellular level of biological organization (Boveri, 1929). After a number of course corrections to accommodate lacks of fit, Boveri's ideas have coalesced into what is now generally accepted as the Somatic Mutation Theory of carcinogenesis (Hanahan and Weinberg, 2000; Mastorides and Maronpot, 2002). Throughout the twentieth century, this theory has been challenged by others, who proposed instead that carcinogenesis takes place at the tissue level of biological organization (Orr, 1958; Smithers, 1962; Hodges et al., 1977; Sonnenschein and Soto, 2000). In the past decade, attempts to find a synthetic position that would incorporate claims from both theoretical approaches have also been advanced (Folkman et al., 2000; Bissell and Radisky, 2001; Thiery, 2002). Objectively, however, the identification of the target(s) upon which the carcinogenic agents act in order to initiate neoplastic transformation has, so far, remained elusive.

The development of mammary cancer in susceptible rodent strains following administration of *N*-nitrosomethylurea (NMU) is a widely accepted model for the study of chemical carcinogenesis (Gullino et al., 1975). The majority of NMU-induced rat mammary tumors are carcinomas or adenocarcinomas, that is tumors of presumed epithelial origin (Thompson, H. J. et al., 2000a). According to the Somatic Mutation Theory, a neoplastic outcome would result from accumulated NMU-induced mutations in one of the epithelial cells of this gland (Guzman et al., 1992; Gould, 1995). Although these carcinomas show an altered organization of both the epithelium and the stroma, when examined through a light microscope, changes observed in the stroma have been assumed to be a secondary effect of the primary mutational events in the epithelium.

An alternative theory considers that carcinogenesis is a process akin to development gone awry (Pierce et al., 1978; Sonnenschein and Soto, 1999a). The Tissue Organization Field Theory proposes that carcinogens alter stromal-epithelial interactions and that proliferation is the default state of all cells (Sonnenschein and Soto, 1999b; Sonnenschein and Soto, 2000). Carcinogenesis would therefore be an emergent phenomenon that takes place at the tissue level of biological organization. As mentioned above, several authors have proposed synthetic approaches that straddle both theories as applied to mammary carcinogenesis (Bissell and Radisky, 2001; Wiseman and Werb, 2002; Thiery, 2002).

In an effort to deal comprehensively and simultaneously with all the competing theories, we decided to use a rat mammary tissue recombination model. This model affords an easy surgical separation of stroma and epithelium such that each compartment might be exclusively exposed to the carcinogen. We chose NMU because it is a direct carcinogen in that it does not need to be metabolized in order to form DNA adducts and has a very short half-life (Swann, 1968). This minimizes the risk of inadvertent indirect exposure of epithelial cells to the carcinogen when recombining them with the stroma. The outcome of the proposed experimental design would determine whether the primary target of NMU is the epithelium (as suggested by the Somatic Mutation Theory), the stroma (as implied by the Tissue Organization Field Theory), or both tissue compartments.

## Materials and Methods

### Chemicals and cell culture reagents

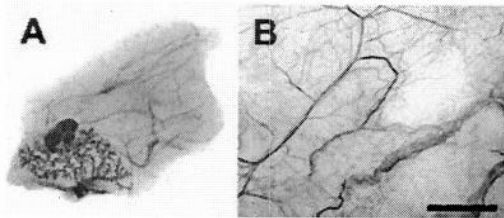
NMU (CAS #684-93-5), insulin, penicillin, progesterone, prolactin, fatty acid-free fraction V bovine serum albumin (BSA), hydrocortisone, human transferrin, ascorbic acid, gentamicin, aluminum potassium sulfate and methyl salicylate were purchased from Sigma-Aldrich. Human epidermal growth factor (EGF) and Matrigel™ were obtained from Becton Dickinson. Phenol red-free DMEM/F12 medium and trypsin were obtained from Gibco. Collagenase was purchased from Worthington Biochemical Corporation and pronase from Calbiochem. Percoll™ was obtained from Amersham Pharmacia Biotech and Carmine from Fisher Scientific.

### Animals

Wistar-Furth rats were purchased from Harlan and housed with food and water ad libitum. Animals were maintained on a 14:10 hours light:dark cycle and care was in accordance with the Guidelines for the Care and Use of Animals and the Tufts-New England Medical Center Institutional Animal Care and Use Committee. When the animals were 21 days old, the mammary epithelium was surgically removed from the 4th and 5th inguinal mammary glands according to procedures outlined previously (DeOme et al., 1959). In each of the animals used in these experiments, the excised epithelium was whole-mounted and observed microscopically to assure that the ductal tree was removed in its entirety and that only a small portion of the fat pad remained attached to it (Fig. 1A).

### Tissue recombination experimental design

The animals with cleared fat pads were distributed into experimental Groups 1-4. At 52 days of age, animals from Groups 1 and 2 received a single intraperitoneal dose of 50 mg NMU/kg body weight dissolved



**Fig. 1.** (A) Whole-mount preparation of an intact mammary gland from a 21-day-old rat showing the ductal tree and lymph nodes. (B) Mammary gland fat pad cleared of epithelium at 21 days of age and excised at the end of the experiment, 11 months later. Bar, 4 mm.

in warm 0.85 g/l NaCl solution (vehicle), pH 5.0; by contrast, Groups 3 and 4 were exposed to just the vehicle. Five days later, 50,000 mammary epithelial cells were injected into the cleared fat pads according to the following experimental design: animals from Groups 1 and 4 received vehicle-treated mammary epithelial cells, and animals from Groups 2 and 3 received NMU-treated mammary epithelial cells. Positive and negative control groups were used. These control groups were intact virgin animals that were age-matched to the animals in Groups 1 to 4. They were not subjected to any surgical manipulation. These animals were treated at 52 days of age with NMU and vehicle, respectively. They were injected at the same time with the animals used in Groups 1 to 4. Intact animals injected with NMU were considered as the positive control for tumor incidence and histopathology of the tumors (Group 5). Animals injected with vehicle were considered as the control for spontaneous tumors and for the normal architecture of the mammary gland (Group 6). Four experiments were performed where all the experimental groups were represented. Animals were excluded from the analyses when no epithelial outgrowths were found in the whole mounts ('no takes') or if they died as a result of surgical complications. The initial (i) and final (f) sample sizes at 9 months after the NMU injection were as follows: Group 1, i=14, f=13; Group 2, i=10, f=8; Group 3, i=12, f=10; Group 4, i=11, f=6.

### Cleared fat pad repopulation

A second set of animals with cleared fat pads was transplanted with 50,000 mammary epithelial cells at 52 days of age. The recombinants were inspected 30, 60 and 90 days later.

### Mammary epithelial cell culture

Mammary epithelial cells were isolated from 50-60-day-old virgin female Wistar-Furth rats using a combination of two previously described protocols (Hahm and Ip, 1990; Imagawa et al., 2000). Briefly, the 4th and 5th inguinal mammary glands were bilaterally excised, minced and digested in phenol red-free DMEM containing 0.15% collagenase III at 37°C for 2 hours with agitation. This digest was centrifuged and the pellet was then treated with 0.05% pronase for 30 minutes at 37°C with agitation. This suspension was filtered through a 530 µm-pore Nitex® filter (Sefar America) and the filtrate was centrifuged at 100 g for 3 minutes (Hahm and Ip, 1990). The pellet was resuspended in 1-2 ml of serum-free medium (SFM) containing phenol red-free DMEM/F12 plus 10 µg/ml insulin, 1 µg/ml progesterone, 10 ng/ml EGF, 1 µg/ml prolactin, 1 mg/ml BSA, 1 µg/ml hydrocortisone, 5 µg/ml human transferrin, 0.88 µg/ml ascorbic acid and 50 µg/ml gentamicin (Hahm and Ip, 1990). This cell suspension was layered over a pre-made Percoll™ gradient (Imagawa et al., 2000) and centrifuged for 20 minutes at 800 g. Single epithelial cells and organoids were recovered from the gradient, diluted in SFM and similarly centrifuged. The pellet was resuspended in SFM and plated on Matrigel™-coated (100 µg/cm<sup>2</sup>) 6-well plates (Becton Dickinson). This layer was enough to promote cell attachment but insufficient to facilitate three-dimensional growth. Non-epithelial cells were successfully removed by treating the plates with a 0.025% trypsin and 0.01% EDTA solution. Five days before being transplanted into recipient animals, the mammary epithelial cells were treated with SFM containing either vehicle or 50 µg/ml NMU for 1 hour at 37°C (Miyamoto et al., 1988). The cells were then rinsed twice with SFM and fresh SFM was added. NMU was used within 5 minutes of preparation. A different batch of mammary epithelial cells prepared following this protocol was used for each of the four experiments. The dose of NMU used in the in vitro experiments was selected following Miyamoto et al. (Miyamoto et al., 1988).

### Epithelial cell transplantation

After harvesting by trypsinization, the cells were counted in a Coulter

Counter Apparatus (Model ZM, Coulter Electronics). The volume of the cell suspension was adjusted in order to inject 50,000 cells in 10  $\mu$ l into the CFP using a Hamilton syringe. All rats receiving a cell transplant were palpated weekly, starting one month after the mammary epithelial cell inoculation. Thoracic glands were used as internal controls for the carcinogen and were equally palpated. Animals were sacrificed when inguinal tumors reached 1 cm in diameter or 9 months after cell transplant, whichever came first.

#### DNA extraction and analysis of Ha-ras-1 gene mutation

DNA was extracted from mammary neoplastic lesions, fat pads and whole mammary glands from virgin rats using the DNeasy kit (Quiagen), following the manufacturer's instructions. We used the mismatch amplification mutation assay (MAMA) described by Cha et al. (Cha et al., 1996) with some modifications. The MAMA is specific for the codon 12 GGA to GAA mutation in Ha-ras-1 gene. Briefly, this method uses two sets of primers; one targets the mutation and the other a control area in the genomic DNA. The mutant-specific mismatch primer PAA (5'-CTTGTGGTGGTGGGCGCTGAA-3'), the Pmnl2 (5'-ACTCGTCCACAAAATGGTTC-3') and the control primers (P1: 5'-CCTGGTTTGGCAACCCTGT-3'; and Pmnl2: 5'-ACTCGTCCACAAAATGGTTC-3') were used at a 40 ng/ $\mu$ l concentration. The PCR was performed using Platinum Supermix (Invitrogen). The PCR products were run in a 2% agarose gel (Gibco). The expected size of the non-mutated Ha-ras-1 gene is 128 bp, whereas the mutated Ha-ras-1 gene is 74 bp.

#### Whole mounts and histology

Whole mounts were prepared following protocols described by the Laboratory of Genetics and Physiology at the National Institute of Diabetes, Digestive and Kidney Diseases within the National Institutes of Health (<http://mammary.nih.gov>), and Thompson et al. (Thompson et al., 1995). The mammary glands were removed and spread on a 75 $\times$ 50 $\times$ 1 mm glass slide (Fisher Scientific), fixed overnight in 10% phosphate-buffered formalin, dehydrated in 70%, 95% and 100% alcohols, cleared in toluene, rehydrated and stained with Carmine Alum. After staining, the whole mounts were dehydrated as described above, cleared in xylene, and bagged in Kpak<sup>®</sup> SealPak heat-seal pouches in methyl salicylate. The whole mounts were analyzed under a stereomicroscope for microscopic lesions. Tumors larger than 0.5 cm were removed before whole mounts were prepared and separately fixed as described above. Microscopic lesions were removed and embedded in paraffin for histological analysis. Images were captured with an AxioCam HR color digital camera (Carl Zeiss) attached to a Stemi 2000 stereomicroscope (Carl Zeiss).

#### Immunohistochemistry

An antigen-retrieval method based on microwave pretreatment and 0.01 M sodium citrate buffer (pH 6) was used as previously described (Maffini et al., 2001). Mouse monoclonal anti-pan cytokeratin (Sigma-Aldrich), anti-vimentin (Novocastra) and anti-desmin (Novocastra) were used at 1:700, 1:100 and 1:100 dilutions, respectively. The antigen-antibody reaction was visualized using the streptavidin-peroxidase complex, with diaminobenzidine tetrahydrochloride (Sigma-Aldrich) as the chromogen. Counterstaining was performed with Harris' hematoxylin. For the double-staining immunofluorescence technique, cytokeratin and vimentin were detected using a previously described technique (Maffini et al., 2002). The primary antibodies were used at 1:100 dilutions in 4% BSA supplemented with 10% normal goat serum. Secondary antibodies and streptavidin-Alexa 594 and 488 (Molecular Probes) were used at 1:100 dilutions. Cell nuclei were counterstained with Hoechst 33258. Images were captured with an AxioCam HR

color digital camera (Carl Zeiss) attached to an Axioskop 2 plus microscope (Carl Zeiss).

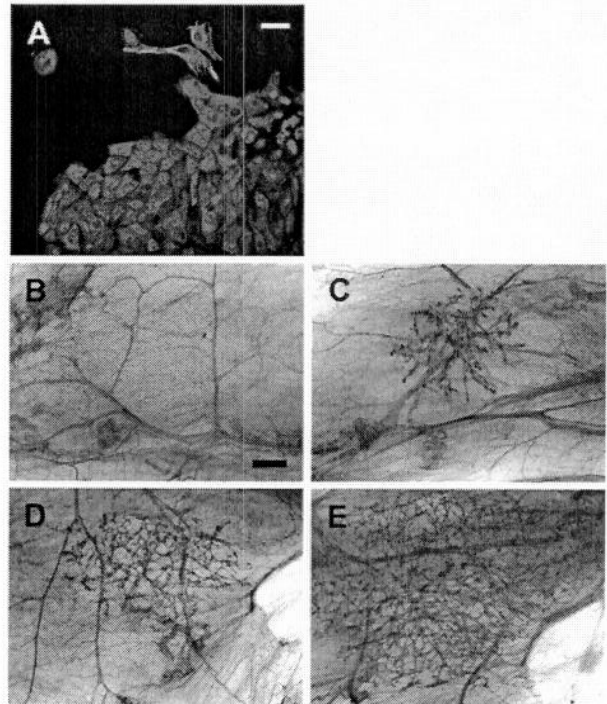
#### Statistics

Statistical significance of the incidence of neoplastic lesions and Ha-ras-1 gene mutation were determined using the  $\chi^2$  Test. The Mann-Whitney and Kruskal-Wallis tests were used to compare the latency periods and the number of lesions in inguinal and thoracic mammary glands between groups. To compare the latency of pectoral and inguinal lesions in the same animal within each treatment group, we used the Wilcoxon signed ranks test, and treated the pectoral and inguinal latency for each animal as a pair.

#### Results

##### Normal ducts developed from cultured mammary epithelial cells

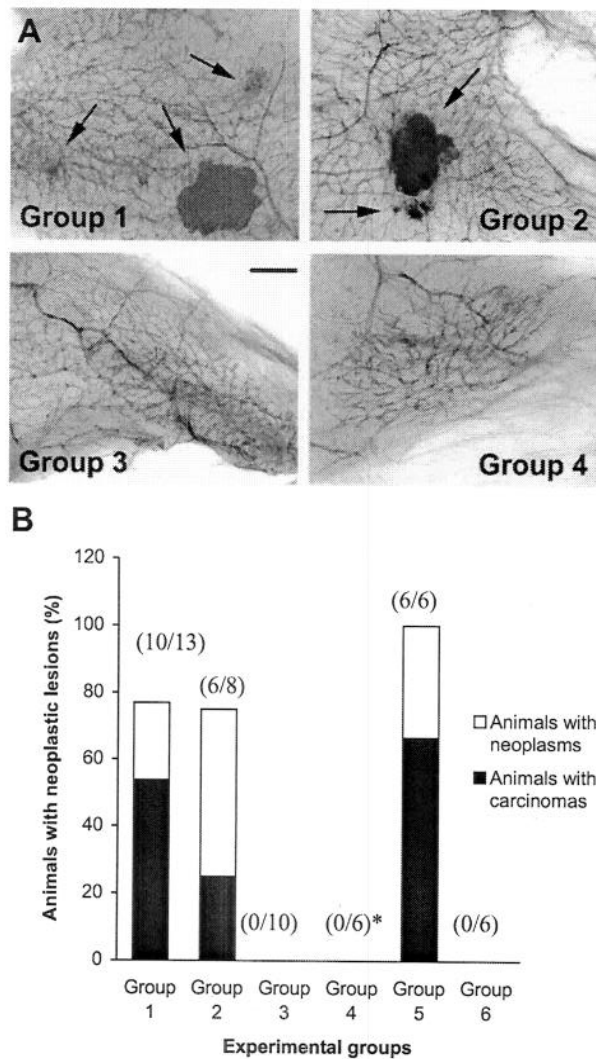
The tissue recombination components were mammary gland stroma (cleared fat pad) and mammary epithelial cells grown in vitro (Fig. 2A). We observed the phenotype of the ductal outgrowth and the repopulation dynamics in the cleared fat pads after transplantation of 50,000 mammary epithelial cells. The ductal outgrowths were phenotypically normal and, 90 days after mammary epithelial cell transplantation, the ductal tree covered a third of the fat pad (Fig. 2B-E).



**Fig. 2.** Repopulation of the mammary gland. (A) Mammary epithelial cells grown in culture showing the expression of cytokeratin (red) and vimentin (green). Mammary epithelial cells averaged 90% of the total cell population transplanted into cleared fat pads. Counterstaining, Hoechst 33258 (blue). Mammary epithelial cells were injected into cleared fat pads and the recombinants were harvested at 0 (B), 30 (C), 60 (D) and 90 (E) days after cell injection. Bars, 20  $\mu$ m (A); 2 mm (B-E).

Neoplastic transformation of mammary epithelial cells

We observed that only those animals whose stroma was exposed to NMU developed neoplasms, regardless of whether or not the transplanted mammary epithelial cells were exposed to the carcinogen (Fig. 3A). The incidence of neoplastic lesions in Groups 1 and 2 was 76.9% (10/13) and 75% (6/8), respectively (Fig. 3B). The positive control Group 5 had 100% incidence (6/6). There were no significant differences in neoplastic incidence between Groups 1 and 2 ( $P=0.920$ ) or between Groups 1 or 2 and Group 5 ( $P=0.200$  and  $P=0.186$ , respectively). By contrast, the animals whose stroma was

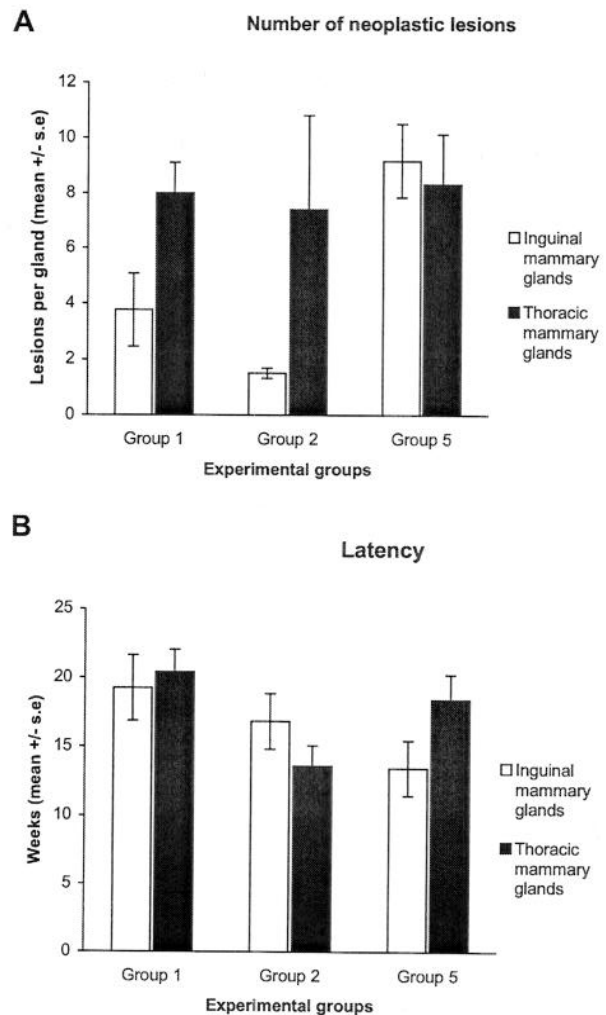


**Fig. 3.** Neoplasms developed in NMU-treated stroma only. (A) Mammary gland whole-mount preparations show abnormal outgrowths in animals whose cleared fat pads were exposed to NMU prior to recombination with vehicle-treated mammary epithelial cells (Group 1) or NMU-treated mammary epithelial cells (Group 2). Neoplastic lesions (arrows) were confirmed histologically. Groups 3 and 4 developed normal-like ductal outgrowths. Bar, 2 mm. (B) Percentage of neoplastic lesions and incidence of carcinomas per experimental group. The number of rats with neoplastic lesions out of the total number of animals in each group is indicated in parenthesis. \*See Materials and Methods for further details.

exposed to vehicle developed no neoplasms, regardless of whether the mammary epithelial cells were exposed in vitro to NMU (Group 3, 0/10) or to vehicle (Group 4, 0/6). The negative control Group 6 had 0% incidence (0/6). Group 3 was significantly different from Group 1 ( $P<0.001$ ) and Group 2 ( $P=0.001$ ). Group 4 was also significantly different from Group 1 ( $P=0.002$ ) and Group 2 ( $P=0.005$ ).

Multiple neoplastic lesions were found

Multiple lesions were observed in the inguinal mammary glands of rats in Groups 1, 2 and 5 (Fig. 4A), suggesting that the neoplasms found in these groups were not a consequence of mechanical injury resulting from the injection procedure. The inguinal glands of Group 5 had twice as many lesions as those in Groups 1 and 2 ( $P=0.013$  and  $P=0.001$ , respectively) (Fig. 4A). This difference might have been owing to the fact that the intact mammary glands in Group 5 had a full complement of epithelium whereas Groups 1 and 2 had an



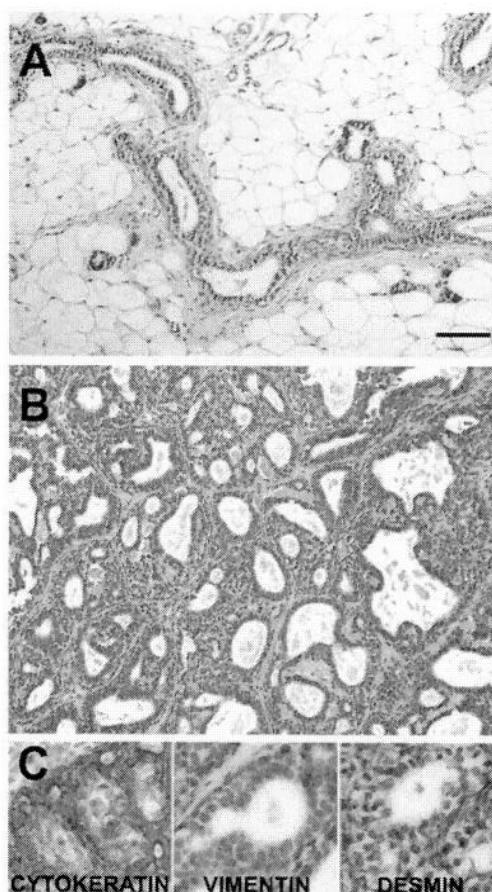
**Fig. 4.** Incidence of neoplasms and latency period. (A) Number of neoplastic lesions in inguinal and thoracic mammary glands (mean±s.e.). (B) Latency of neoplastic lesions in inguinal and thoracic mammary glands expressed in weeks (mean±s.e.).

initial population of only 50,000 mammary epithelial cells. The incidence of neoplastic lesions in the thoracic mammary glands of NMU-treated rats from Groups 1, 2 and 5 was comparable ( $P=0.622$ ) (Fig. 4A). There was no significant difference among Groups 1, 2 and 5 regarding inguinal tumor latency periods ( $P=0.147$ ). The latency period was similar in the thoracic and inguinal mammary glands within the same experimental groups (Group 1:  $P=0.276$ ; Group 2:  $P=0.414$ ; Group 5:  $P=0.684$ ) (Fig. 4B).

We performed the histopathological analyses of the neoplastic lesions following the classification described by Russo et al. (Russo et al., 1990). Carcinomas were seen in 53.8% of the animals from Group 1, 25% of Group 2 and 66.7% of Group 5 (Fig. 3B), and represented 70%, 33% and 66.7% of the neoplasms found in these groups, respectively (Table 1). The most frequent type of neoplastic lesion was papillary carcinoma (Fig. 5B, Table 1). All the tumors were of epithelial origin; the neoplastic cells were cytokeratin positive, and vimentin and desmin negative (Fig. 5C). Regardless of whether or not the mammary epithelial cells had been exposed to NMU, the tissue-recombined mammary glands of animals that did not develop tumors appeared histologically similar to a normal mammary gland (Fig. 5A).

#### Mutated *Ha-ras-1* does not correlate with neoplasia

We analyzed the DNA of neoplastic lesions from Groups 1 and 2 and observed that 2 out of 11 neoplasms from Group 1, and 1 out of 6 from Group 2, lacked the G-A mutation in the codon 12 of the *Ha-ras-1* gene. Similarly, DNA taken from the neoplastic lesions in the positive control (Group 5) showed that 1 out of 7 lacked the point mutation (Fig. 6). No statistically significant difference was found between the groups ( $P=0.977$ ). In order to test whether any correlation existed between the presence of the mutated *Ha-ras-1* gene and the initiation of neoplasia, we analyzed DNA extracted from the stroma of animals treated with vehicle (i.e. Groups 3 and 4). All stroma samples from Groups 3 (7 out of 7) and 4 (6 out of 6) showed the mutation. Thus, we now report that this *Ha-ras-1* gene mutation was present in the mammary gland fat pad of rats exposed to vehicle. Moreover, DNA harvested from whole mammary glands of intact rats randomly taken from our colony



**Fig. 5.** Sections of recombinant tissues. (A) Section from a recombinant of vehicle-exposed stroma and NMU-exposed mammary epithelial cells. The histoarchitecture resembles a normal mammary gland. (B) Papillary carcinoma from a recombinant of NMU-exposed stroma and vehicle-exposed mammary epithelial cells. Hematoxylin and eosin staining (A,B). (C) Immunohistochemistry for cytokeratin, vimentin and desmin in sections of the tumor shown in B. Counterstaining: Harris' hematoxylin. Bar, 100  $\mu$ m.

**Table 1. Incidence of mammary neoplastic lesions in groups exposed to NMU**

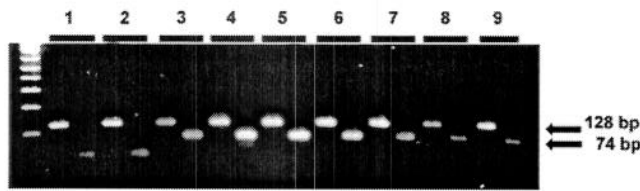
Experimental group	Histopathological classification	Incidence (%) <sup>*</sup>
Group 1	Carcinomas	70
	Papillomas	10
	Cystoadenomas	10
	Adenomas	10
Group 2	Carcinomas	33.3
	Papillomas	16.7
	Fibroadenomas	33.3
	Fibroma	16.7
Group 5 (Positive control)	Carcinomas	66.7
	Adenomas	16.7
	Cystoadenomas	16.6

<sup>\*</sup>The number of neoplastic lesions in each histological category was divided by the total number of lesions observed in each experimental group

(4 out of 4) also showed the mutation, which agrees with previous findings (Cha et al., 1996). The incidence of mutated *Ha-ras-1* gene was not significantly different between animals that were or were not exposed to NMU ( $P=0.604$ ). Finally, the mutation was also assessed in DNA isolated from mammary epithelial cells, mammary fibroblasts, and mammary pre-adipocytes collected from intact virgin rats and grown in vitro. All these different types of cells were collected at different times during the course of 2 years. DNA was extracted from frozen cells, vehicle-treated cells and NMU-treated cells. The presence of the mutation did not correlate with cell type, culture conditions or carcinogen treatment (data not shown).

#### Discussion

Our results regarding the role of histoarchitecture in carcinogenesis are consistent with previous findings stemming from the use of diverse rodent models. Barcellos-Hoff and



**Fig. 6.** Analysis of the presence of point mutation in the *Ha-ras-1* gene using the MAMA. The mutant-specific amplification product is 74 bp whereas the normal product is 128 bp. Lanes 1, 5, 6 and 7: mammary tumors from Group 5. Tumor in lane 1 lacks *Ha-ras-1* gene mutation. Lane 2: mammary tumor from Group 1. Note absence of *Ha-ras-1* gene mutation. Lanes 3 and 4: mammary tumors from Group 2. Lanes 8 and 9: normal mammary tissue from intact animals taken randomly from the colony. Note: the smaller bands in lanes 1 and 2 correspond to dimers of the primer.

Ravani showed that radiation-induced changes in the stromal microenvironment contributed to the neoplastic progression of non-irradiated, quasi-normal, established COMMA-1 mammary epithelial cells (Barcellos-Hoff and Ravani, 2000). Sternlicht et al. observed that overexpression of the matrix metalloproteinase stromelysin-1 can induce carcinogenesis in mouse mammary glands (Sternlicht et al., 1999). Also, using tissue recombinant techniques, Olumi et al. concluded that 'primary, phenotypically normal fibroblasts associated with a human epithelial malignancy can stimulate progression of a nontumorigenic (prostate) epithelial cell' (Olumi et al., 1999). Thompson et al. have also used a tissue recombination model, the mouse prostate reconstitution model system, and observed that 'intrinsic properties of the BALB/c mesenchyme can arrest the progression of *ras+myc*-initiated C57BL/6 epithelium from benign hyperplasia to malignant carcinoma' (Thompson et al., 1993).

Our experiments, designed to explore simultaneously the competing theories mentioned in the introduction, suggest that the stroma is a target of NMU in mammary carcinogenesis. We were concerned, of course, that inadvertent technical mishaps might have influenced our data. For instance, epithelial cells might have remained in the fat pads after the clearing procedure and could have been exposed *in vivo* to NMU. We addressed this possibility by microscopically examining the tissue containing the ductal tree after clearing the fat pads at 21 days of age and verifying that the margins contained no epithelial cells (Fig. 1A). In addition, we also cleared the 5th mammary gland to prevent the migration of indigenous epithelial cells into the 4th cleared fat pad. Therefore, we consider it unlikely that epithelial cells were present after clearing. It was also reassuring to observe that cleared fat pads not injected with mammary epithelial cells remained free of epithelium at the end of the experiment (Fig. 1B).

Several research groups have used experimental rodent models to explore the concept that epithelial cells are the targets of carcinogens, as implied by the Somatic Mutation Theory. Miyamoto et al. reported tumor formation after mammary epithelial cells were exposed to NMU *in vitro* and injected into cleared fat pads (Miyamoto et al., 1988). These authors used a cell inoculum one order of magnitude higher than the one we used and a different cell purification method. Also, they added the NMU when the cultures were 3 days old

and made no reference to the degree of fibroblast contamination. It is conceivable that, in their experiments, fibroblasts exposed to NMU *in vitro* could have played a role in the carcinogenic process. On the contrary, we repeatedly trypsinized and subcultured the mammary epithelial cells to enrich this pool of cells and reduce fibroblast contamination. In essence, we exposed a highly enriched mammary epithelial cell population to NMU (Fig. 2A). Furthermore, Miyamoto et al. injected the mammary epithelial cells into fat pads immediately after clearing, while in the midst of wound healing (Miyamoto et al., 1988). In this context, it has been shown that carcinogenesis is promoted by a wounded stroma (Konstantinidis et al., 1982; Sieweke et al., 1990). Their data and those by Guzman et al. do not suggest a positive correlation between tumor yield and either NMU concentration or the number of exposures to this carcinogen *in vitro*. Moreover, normal epithelial outgrowths were observed at all NMU doses (Guzman et al., 1987; Miyamoto et al., 1988). Using yet another protocol, Kamiya et al. showed that NMU- or radiation-exposed mammary epithelial cells yielded mammary carcinomas when grafted into rat fat pads that were 'cleared' by injecting 70% ethanol (Kamiya et al., 1995). They interpreted these data as evidence that tumor formation was due to undefined epigenetic factors rather than to mutations. They also observed that tumor incidence diminished as the number of cells injected increased, an outcome inconsistent with the Somatic Mutation Theory.

These experiments dealing with *in vitro* exposure to NMU were based on the premise that NMU acted directly on the epithelial cells and, therefore, under this rationale, no attempt was made to evaluate the role of the stroma in tumor formation (Greiner et al., 1983; Guzman et al., 1987; Miyamoto et al., 1988; Delp et al., 1990). The novelty of our observations stems from the fact that a carcinogen-treated stroma was able to transform vehicle-treated cells into neoplastic tissues comparable with those seen in intact NMU-exposed rats (positive control Group 5) (Fig. 5 and Table 1).

The prevalent hypothesis that NMU exposure results in carcinogenesis because of NMU-induced point mutations in the codon 12 of the *Ha-ras-1* gene of mammary epithelial cells (Zarbl et al., 1985) has been challenged. As shown in our results and in the literature (Cha et al., 1994; Cha et al., 1996; Swanson et al., 1996; Shirai et al., 1997; Thompson, T. A. et al., 2000b), not all NMU-induced mammary neoplasms express this mutation. Also, Korkola and Archer have observed comparable results in NMU-induced pre-neoplastic lesions (Korkola and Archer, 1999). Equally important, this mutation is present in mammary glands from non-exposed animals (Cha et al., 1996). Here, we confirm these findings and show that the frequency of tumors expressing mutated *Ha-ras-1* is statistically similar in the positive controls (Group 5) and recombinants from NMU-exposed stroma (Groups 1 and 2). Moreover, we also observed that mutated *Ha-ras-1* is also present in the cleared mammary fat pad of vehicle-exposed animals. Furthermore, Zhang et al. demonstrated that increasing the dose of NMU increased total tumor yield but reduced the frequency of mammary tumors expressing mutated *Ha-ras-1* (Zhang et al., 1990). In sum, these data suggest that the *Ha-ras-1* gene mutation appears to be neither necessary nor sufficient for neoplastic transformation and that it is not exclusively present in the epithelial cells.

The concept that altered tissue architecture is at the core of carcinogenesis was pioneered by Waddington (Waddington, 1935), Orr (Orr, 1958) and, more recently, by Bissell and Radisky (Bissell and Radisky, 2001) and others (Sonnenschein and Soto, 2000; Moss, 2003; Weaver and Gilbert, 2004). Altogether, our data and those of others challenge the long-held notion that carcinogens induce mammary cancer by causing mutations in the DNA of an epithelial cell (Fearon and Vogelstein, 1990; Mastorides and Maronpot, 2002). These results suggest the need to explore the roles that the stroma components [i.e. the cells (fibroblasts, adipocytes, mast cells, etc.)] and the extracellular matrix play in rodent mammary carcinogenesis. Efforts should also be directed at exploring the role of the stroma in experimental models for carcinogenesis involving organs other than the mammary gland (i.e. skin, prostate, liver, bladder). To accommodate a novel perspective on the role of the stroma in carcinogenesis, a rigorous analysis of concepts, definitions and experimental approaches is now needed. This will facilitate the identification of the mediators responsible for the altered tissue phenotype in cancers and of ways to reverse their effect by adopting a solid epigenetic perspective.

A report on these findings was made at the 12th International Conference of the International Society of Differentiation, 14-17 September 2002, at Lyon, France. This research was supported primarily by the Bradshaw Foundation (Geneva, Switzerland), by the USA Department of Defense grant 17-01-1-0654 and by the Massachusetts Department of Public Health. Dr Will Rand's statistical advice is appreciated, as is the technical help of Dr Peter Geck, Jenny Lenkowski, Cheryl Michaelson and Carise Wieloch. The authors also thank Drs D. Radinsky, P. Kenny, T. Shioda and J. Russo for their critical reading of the manuscript.

## References

- Barcellos-Hoff, M. H. and Ravani, S. A. (2000). Irradiated mammary gland stroma promotes the expression of tumorigenic potential by unirradiated epithelial cells. *Cancer Res.* **60**, 1254-1260.
- Bissell, M. J. and Radisky, D. (2001). Putting tumours in context. *Nat. Rev. Cancer* **1**, 46-54.
- Boveri, T. (1929). *The Origin of Malignant Tumors*. Baltimore: Williams & Wilkins.
- Cha, R. S., Thilly, W. G. and Zarbl, H. (1994). *N*-nitroso-*N*-methylurea-induced rat mammary tumors arise from cells with preexisting oncogenic Hras1 gene mutations. *Proc. Natl. Acad. Sci. USA* **91**, 3749-3753.
- Cha, R. S., Guerra, L., Thilly, W. G. and Zarbl, H. (1996). Ha-ras-1 oncogene mutations in mammary epithelial cells do not contribute to initiation of spontaneous mammary tumorigenesis in rats. *Carcinogenesis* **17**, 2519-2524.
- Delp, C., Treves, J. and Banerjee, M. (1990). Neoplastic transformation and DNA damage of mouse mammary epithelial cells by *N*-methyl-*N*-nitrosourea in organ culture. *Cancer Lett.* **55**, 31-37.
- DeOme, K. B., Faulkin, L. J., Jr, Bern, H. A. and Blair, P. B. (1959). Development of mammary tumors from hyperplastic alveolar nodules transplanted into gland-free mammary fat pads of female C3H mice. *Cancer Res.* **19**, 515-525.
- Fearon, E. and Vogelstein, B. (1990). A genetic model for colorectal tumorigenesis. *Cell* **61**, 759-767.
- Folkman, J., Hahnfeldt, P. and Hlatky, L. (2000). Cancer: looking outside the genome. *Nat. Rev. Mol. Cell Biol.* **1**, 76-79.
- Gould, M. N. (1995). Rodent models for the study of etiology, prevention and treatment of breast cancer. *Semin. Cancer Biol.* **6**, 147-152.
- Greiner, J. W., DiPaolo, J. A. and Evans, C. H. (1983). Carcinogen-induced phenotypic alterations in mammary epithelial cells accompanying the development of neoplastic transformation. *Cancer Res.* **43**, 273-278.
- Gullino, P. M., Pettigrew, H. M. and Grantham, F. H. (1975). *N*-nitrosomethylurea as mammary gland carcinogen in rats. *J. Natl. Cancer Inst.* **54**, 401-414.
- Guzman, R. C., Osborn, R. C., Bartley, J. C., Imagawa, W., Asch, B. B. and Nandi, S. (1987). In vitro transformation of mouse mammary epithelial cells grown serum-free inside collagen gels. *Cancer Res.* **47**, 275-280.
- Guzman, R. C., Osborn, R. C., Swanson, S. M., Sakthivel, R., Hwang, S. I., Miyamoto, S. and Nandi, S. (1992). Incidence of c-Ki-ras activation in *N*-methyl-*N*-nitrosourea-induced mammary carcinomas in pituitary-isografted mice. *Cancer Res.* **52**, 5732-5737.
- Hahm, H. A. and Ip, M. M. (1990). Primary culture of normal rat mammary epithelial cells within a basement membrane matrix. I. Regulation of proliferation by hormones and growth factors. *In Vitro Cell. Dev. Biol.* **26**, 791-802.
- Hanahan, D. and Weinberg, R. A. (2000). The hallmarks of cancer. *Cell* **100**, 57-70.
- Hodges, G. M., Hicks, R. M. and Spacey, G. D. (1977). Epithelial-stromal interactions in normal and chemical carcinogen-treated adult bladder. *Cancer Res.* **37**, 3720-3730.
- Imagawa, W., Yang, J., Guzman, R. C. and Nandi, S. (2000). Collagen gel method for the primary culture of mouse mammary epithelium. In *Methods in Mammary Gland Biology and Breast Cancer Research* (ed. M. M. Ip and B. B. Asch), pp. 111-123. New York: Kluwer.
- Kamiya, K., Yasukawa-Barnes, J., Mitchen, J. M., Gould, M. N. and Clifton, K. H. (1995). Evidence that carcinogenesis involves an imbalance between epigenetic high-frequency initiation and suppression of promotion. *Proc. Natl. Acad. Sci. USA* **92**, 1332-1336.
- Konstantinidis, A., Smulow, J. B. and Sonnenschein, C. (1982). Tumorigenesis at a predetermined oral site after one intraperitoneal injection of *N*-nitroso-*N*-methylurea. *Science* **216**, 1235-1237.
- Korkola, J. E. and Archer, M. C. (1999). Resistance to mammary tumorigenesis in Copenhagen rats is associated with the loss of preneoplastic lesions. *Carcinogenesis* **20**, 221-227.
- Maffini, M. V., Ortega, H., Stoker, C., Giardina, R., Luque, E. H. and Munoz de Toro, M. M. (2001). Bcl-2 correlates with tumor ploidy and nuclear morphology in early stage prostate carcinoma. *Pathol. Res. Pract.* **197**, 487-492.
- Maffini, M. V., Geck, P., Powell, C. E., Sonnenschein, C. and Soto, A. M. (2002). Mechanism of androgen action on cell proliferation AS3 protein as a mediator of proliferative arrest in the rat prostate. *Endocrinology* **143**, 2708-2714.
- Mastorides, S. and Maronpot, R. R. (2002). Carcinogenesis. In *Handbook of Toxicologic Pathology*, 2nd edn (ed. W. M. Haschek-Hock, C. G. Rousseaux and M. A. Wallig), pp. 83-122. Urbana: Academic Press.
- Miyamoto, S., Guzman, R. C., Osborn, R. C. and Nandi, S. (1988). Neoplastic transformation of mouse mammary epithelial cells by in vitro exposure to *N*-methyl-*N*-nitrosourea. *Proc. Natl. Acad. Sci. USA* **85**, 477-481.
- Moss, L. (2003). *What Genes Can't Do*. Cambridge: MIT Press.
- Olumi, A. F., Grossfeld, G. D., Hayward, S. W., Carroll, P. R., Tlsty, T. D. and Cunha, G. R. (1999). Carcinoma-associated fibroblasts direct tumor progression of initiated human prostatic epithelium. *Cancer Res.* **59**, 5002-5011.
- Orr, J. W. (1958). The mechanism of chemical carcinogenesis. *Br. Med. Bull.* **14**, 99-101.
- Pierce, G. B., Shikes, R. and Fink, L. M. (1978). *Cancer: A Problem of Developmental Biology*. Englewoods Cliffs: Prentice-Hall.
- Russo, J., Russo, I. H., Rogers, A. E., van Zwieten, M. J. and Gusterson, B. A. (1990). Tumours of the mammary gland. In *Pathology of Tumours in Laboratory Animals. Vol 1. Tumors of the Rat*, 2nd edn (ed. V. S. Turusov and U. Mohr), pp. 47-78. Lyon: IARC Scientific Publication N 99.
- Shirai, K., Uemura, Y., Fukumoto, M., Tsukamoto, T., Pascual, R., Nandi, S. and Tsubura, A. (1997). Synergistic effect of MNU and DMBA in mammary carcinogenesis and H-ras activation in female Sprague-Dawley rats. *Cancer Lett.* **120**, 87-93.
- Sieweke, M. H., Thompson, N. L., Sporn, M. B. and Bissell, M. J. (1990). Mediation of wound-related Rous sarcoma virus tumorigenesis by TGF-beta. *Science* **248**, 1656-1660.
- Smithers, D. W. (1962). Cancer: an attack of cytologism. *Lancet* **1**, 493-499.
- Sonnenschein, C. and Soto, A. M. (1999a). *The Society of Cells: Cancer and Control of Cell Proliferation*. New York: Springer-Verlag.
- Sonnenschein, C. and Soto, A. M. (1999b). The enormous complexity of cancer. In *The Society of Cells: Cancer and Control of Cell Proliferation*, pp. 99-111. New York: Springer-Verlag.



- Sonnenschein, C. and Soto, A. M.** (2000). The somatic mutation theory of carcinogenesis: Why it should be dropped and replaced. *Mol. Carcinog.* **29**, 1-7.
- Sternlicht, M. D., Lochter, A., Sympson, C. J., Huey, B., Rougier, J. P., Gray, J. W., Pinkel, D., Bissell, M. J. and Werb, Z.** (1999). The stromal proteinase MMP3/Stromelysin-1 promotes mammary carcinogenesis. *Cell* **98**, 137-146.
- Swann, P. F.** (1968). The rate of breakdown of methyl methanesulphonate, dimethyl sulphate and *N*-methyl-*N*-nitrosourea in the rat. *Biochem. J.* **110**, 49-52.
- Swanson, S. M., Guzman, R. C., Tsukamoto, T., Huang, T. T., Dougherty, C. D. and Nandi, S.** (1996). *N*-Ethyl-*N*-nitrosourea induces mammary cancers in the pituitary-isografted mouse which are histologically and genotypically distinct from those induced by *N*-methyl-*N*-nitrosourea. *Cancer Lett.* **102**, 159-165.
- Thiery, J. P.** (2002). Epithelial-mesenchymal transitions in tumour progression. *Nat. Rev. Cancer* **2**, 442-454.
- Thompson, H. J., McGinley, J. N., Rothhammer, K. and Singh, M.** (1995). Rapid induction of mammary intraductal proliferations, ductal carcinoma in situ and carcinomas by the injection of sexually immature female rats with 1-methyl-1-nitrosourea. *Carcinogenesis* **16**, 2407-2411.
- Thompson, H. J., Singh, M. and McGinley, J.** (2000). Classification of premalignant and malignant lesions developing in the rat mammary gland after injection of sexually immature rats with 1-methyl-1 nitrosourea. *J. Mammary Gland Biol. Neoplasia* **5**, 201-210.
- Thompson, T. A., Haag, J. D. and Gould, M. N.** (2000). *ras* gene mutations are absent in NMU-induced mammary carcinomas from aging rats. *Carcinogenesis* **21**, 1917-1922.
- Thompson, T. C., Timme, T. L., Kadmon, D., Park, S. H., Egawa, S. and Yoshida, K.** (1993). Genetic predisposition and mesenchymal-epithelial interactions in *ras*+*myc*-induced carcinogenesis in reconstituted mouse prostate. *Mol. Carcinog.* **7**, 165-179.
- Waddington, C. H.** (1935). Cancer and the theory of organizers. *Nature* **135**, 606-608.
- Weaver, V. M. and Gilbert, P.** (2004). Watch thy neighbor: cancer is a communal affair. *J. Cell. Sci.* **117**, 1287-1290.
- Wiseman, B. S. and Werb, Z.** (2002). Stromal effects on mammary gland development and breast cancer. *Science* **296**, 1046-1049.
- Zarbl, H., Sukumar, S., Arthur, A. V., Martin-Zanca, D. and Barbacid, M.** (1985). Direct mutagenesis of Ha-*ras*-1 oncogenes by *n*-nitroso-*N*-methylurea during initiation of mammary carcinogenesis in rats. *Nature* **315**, 382-385.
- Zhang, R., Haag, J. D. and Gould, M. N.** (1990). Reduction in the frequency of activated *ras* oncogenes in rat mammary carcinomas with increasing *N*-methyl-*N*-nitrosourea doses or increasing prolactin levels. *Cancer Res.* **50**, 4286-4290.

*(American Journal of Pathology. 2005;166:1405-1418.)*

© 2005 American Society for Investigative Pathology

## Expression of Smad7 in Mouse Eyes Accelerates Healing of Corneal Tissue after Exposure to Alkali

Shizuya Saika<sup>\*</sup>, Kazuo Ikeda<sup>†</sup>, Osamu Yamanaka<sup>\*</sup>,  
Takeshi Miyamoto<sup>\*</sup>, Yoshitaka Ohnishi<sup>\*</sup>, Misako Sato<sup>‡</sup>,  
Yasuteru Muragaki<sup>‡</sup>, Akira Ooshima<sup>‡</sup>, Yuji Nakajima<sup>‡</sup>,  
Winston W.-Y. Kao<sup>§</sup>, Kathleen C. Flanders<sup>¶</sup> and  
Anita B. Roberts<sup>¶</sup>

From the Departments of Ophthalmology<sup>\*</sup> and Pathology,<sup>†</sup> Wakayama Medical University, Wakayama, Japan; the Department of Anatomy,<sup>‡</sup> Graduate School of Medicine, Osaka City University, Osaka, Japan; the Department of Ophthalmology,<sup>§</sup> University of Cincinnati Medical Center, Cincinnati, Ohio; and the Laboratory of Cell Regulation and Carcinogenesis,<sup>¶</sup> National Cancer Institute, National Institutes of Health, Bethesda, Maryland

### ► Abstract

Damage to the cornea from chemical burns is a serious clinical problem that often leads to permanent visual impairment. Because transforming growth factor (TGF)- $\beta$  has been implicated in the response to corneal injury, we evaluated the effects of altered TGF- $\beta$  signaling in a corneal alkali burn model using mice treated topically with an adenovirus (Ad) expressing inhibitory Smad7 and mice with a targeted deletion of the TGF- $\beta$ /activin signaling mediator Smad3. Expression of exogenous Smad7 in burned corneal tissue resulted in reduced activation of Smad signaling and nuclear factor- $\kappa$ B signaling via RelA/p65. Resurfacing of the burned cornea by conjunctival epithelium and its differentiation to cornea-like epithelium were both accelerated in Smad7-Ad-treated corneas with suppressed stromal ulceration, opacification, and neovascularization 20 days after injury. Introduction of the Smad7 gene suppressed invasion of monocytes/macrophages and expression of monocyte/macrophage chemotactic protein-1, TGF- $\beta$ 1, TGF- $\beta$ 2, vascular endothelial growth factor, matrix metalloproteinase-9, and tissue inhibitors of metalloproteinase-2 and abolished the generation of myofibroblasts. Although acceleration of healing of the burned cornea was also observed in mice lacking Smad3, the effects on epithelial and stromal healing were less pronounced than those in

### This Article

- [Abstract](#) **FREE**
- [Full Text \(PDF\)](#)
- [Purchase Article](#)
- [View Shopping Cart](#)

### Services

- [Similar articles in this journal](#)
- [Similar articles in PubMed](#)
- [Alert me to new issues of the journal](#)
- [Download to citation manager](#)
- [Cited by other online articles](#)

### Google Scholar

- [Articles by Saika, S.](#)
- [Articles by Roberts, A. B.](#)
- [Articles citing this Article](#)

### PubMed

- [PubMed Citation](#)
- [Articles by Saika, S.](#)
- [Articles by Roberts, A. B.](#)

- |   |
|---|
| <ul style="list-style-type: none"> <li>▲ <a href="#">Top</a></li> <li>▪ <a href="#">Abstract</a></li> <li>▼ <a href="#">Materials and Methods</a></li> <li>▼ <a href="#">Results</a></li> <li>▼ <a href="#">Discussion</a></li> <li>▼ <a href="#">References</a></li> </ul> |
|---|

corneas treated with Smad7. Together these data suggest that overexpression of Smad7 may have effects beyond those of simply blocking Smad3/TGF- $\beta$  signaling and may represent an effective new strategy for treatment of ocular burns.

---

The cornea is a highly organized avascular transparent tissue located in the anterior part of the eye. It must remain transparent to refract light properly. Ocular trauma in the form of an alkali burn to the cornea is a serious clinical problem and may cause severe and permanent visual impairment.<sup>1</sup> Activation of corneal cells, ie, keratocytes and epithelial cells, and influx of inflammatory cells such as monocytes/macrophages, are both involved in the pathogenesis of injury after alkali tissue damage in the cornea and can lead to persistent epithelial defects.<sup>2,3</sup> Moreover, breakdown of the basement membrane by matrix metalloproteinases (MMPs, gelatinases) secreted by these cells contributes to the pathogenic ulceration and perforation of the stroma.<sup>4-9</sup> Conjunctivalization of the corneal surface on the loss of limbal stem cells together with opacification and neovascularization of the corneal stroma all impair the patients' vision in the later healing phases.<sup>10,11</sup> Surgical transplantation of autografts or allografts of limbal epithelium containing corneal epithelial stem cells is used in some cases.<sup>12,13</sup> Although such allografting can be effective in cases with alkali injury to both eyes, this therapy requires long-term immunosuppression by drugs, potentially increasing risks of infection and producing other unwanted side effects. Moreover, even this treatment is not effective in severe cases, leading to loss of vision, and emphasizing the need for development of new, more effective, treatment strategies.

A number of growth factors and cytokines are believed to be involved in the tissue destruction and late scarring that occur in the cornea after alkali burn. One prime candidate is transforming growth factor (TGF)- $\beta$ , which has been shown not only to promote migration of corneal epithelial cells and keratocytes, but also to be chemotactic to monocytes/macrophages and to induce transdifferentiation of keratocytes to myofibroblasts.<sup>14-17</sup> Overexpression of TGF- $\beta$  in the burned cornea exacerbates damage of the injured tissue, in part by its ability to induce expression of other cytokines, such as vascular endothelial growth factor (VEGF) and monocyte/macrophage chemotactic protein-1 (MCP-1),<sup>18,19</sup> which are believed to be involved in local neovascularization and inflammation, respectively.<sup>20-27</sup>

TGF- $\beta$  activates multiple signaling cascades including those involving the mitogen-activated protein kinase (MAPK), c-Jun-N-terminal kinase, p38MAPK, and Smads.<sup>28-31</sup> Of these, the Smad2/3/4 pathway is uniquely specific for the TGF- $\beta$ /activin signaling.<sup>28-31</sup> In this pathway, receptor-activated Smad proteins, Smad2 or Smad3, are phosphorylated directly by the TGF- $\beta$  type I receptor kinase (T $\beta$ RI), partner with the common mediator, Smad4, and translocate to the nucleus where they play a prominent role in activation of TGF- $\beta$ /Smad-dependent gene targets. Smad3 signaling has been shown to be critical in healing of cutaneous wounds and in injury-induced fibrosis in many tissues, such as skin, kidney, and the lens and retina of the eye.<sup>17,32-40</sup> Smad7 is an inhibitory Smad, inducible not only by TGF- $\beta$  but also by inflammatory cytokines.<sup>28-31</sup> It both blocks Smads2/3 signaling<sup>41,42</sup> and has other putative Smad-independent effects.<sup>43</sup> Transient introduction of the Smad7 gene by using an adenovirus vector has been reported to be effective in treating tissue inflammatory/fibrotic disorders in lung, kidney, liver, and lens of the eye.<sup>44-47</sup> Crosstalk between the Smad and nuclear factor (NF)- $\kappa$ B signal transduction pathways has also been reported.<sup>48-51</sup> In particular, Smad7 has been shown to exert an inhibitory effect on NF- $\kappa$ B

signaling independent of its action on Smad signaling,<sup>52</sup> and might contribute to modulation of the inflammatory reaction triggered by various cytokines. Based on this, we hypothesized that overexpression of Smad7 might simultaneously modulate TGF- $\beta$  and NF- $\kappa$ B signaling pathways and prevent the tissue destruction resulting from alkali injury to the cornea.

To test this hypothesis, we used a mouse model of total ocular surface burn in which the eye is exposed to alkali. Here we show for the first time the therapeutic efficacy of Smad7 adenoviral-mediated cDNA transfer to the alkali-burned mouse cornea. Evaluation of epithelial healing, stromal repair, influx of inflammatory cells, and patterns of cytokine expression all suggest that gene transfer of Smad7 improves the healing of the injured tissue, and reduces scarring and neovascularization. Combined *in vivo* and *in vitro* data demonstrate effects of Smad7 overexpression on both Smad2/3 and NF- $\kappa$ B signaling. The better outcome of eyes treated with Smad7 compared to eyes in Smad3-null mice after alkali injury to the cornea suggests that Smad7 likely affects multiple signaling pathways in addition to those mediated by Smad3.

## ► Materials and Methods

All experimental procedures were approved by the DNA Recombination Experiment Committee and Animal Care and the Use Committee of Wakayama Medical University, Wakayama, Japan, and conducted in accordance with the Association for Research in Vision and Ophthalmology Statement for the Use of Animals in Ophthalmic and Vision Research.

▲ Top
▲ Abstract
▪ Materials and Methods
▼ Results
▼ Discussion
▼ References

### *Adenovirus Vector Construction and Virus Purification*

We used the adenovirus Cre/LoxP-regulated expression vector set (no. 6151; Takara, Tokyo, Japan) to make recombinant adenovirus expressing *Smad7* as previously reported.<sup>44</sup> Each adenoviral vector was used at the concentration of  $1.0 \times 10^7$  PFU/ $\mu$ l.

### *Alkali Burn in C57BL/6 Mice and Treatment with Smad7 Gene Transfer for Histological Evaluation*

Three  $\mu$ l of 1 N sodium hydroxide solution was applied to the right eye of adult C57BL/6 mice ( $n = 87$ ) to produce an ocular surface alkali burn under both general and topical anesthesia.<sup>49</sup> A mixture of recombinant adenoviruses carrying CAG (cytomegalovirus enhancer, chicken  $\beta$ -actin promoter plus a part of 3' untranslated region of rabbit  $\beta$ -globin) promoter-driven Cre (Cre-Ad) and mouse *Smad7* cDNA (Smad7-Ad) was administered at 2 and 24 hours and days 5, 10, and 15 after an alkali exposure (Smad7-Ad group). Cre recombinase expressed via the CAG promoter deletes the stuffer PolyA through the Cre/LoxP system. Preliminary experiments showed that there was no obvious difference in the histology or in healing at the macroscopic level in an alkali-burned mouse eye with (Cre-Ad group) or without application of adenovirus carrying Cre (no vector group). Thus corneas of the Cre-Ad group were used as controls. After the evaluation of the corneal surface with fluorescein staining of the injured

epithelium, the eye globe was enucleated 2 hours after labeling with bromodeoxyuridine (BrdU)<sup>53</sup> and processed for histological examination in either paraffin or cryosections at days 3, 5, 10, and 20. Fluorescein staining of the cornea allows surface defects to be visualized as green. The numbers of eyes for paraffin sections were 4 and 4 (day 3), 6 and 6 (day 5), 14 and 17 (day 10), or 8 and 8 (day 20) in the Cre-Ad and Smad7-Ad groups, respectively. The numbers of eyes for cryosection were two and two (day 3), three and two (day 5), four and three (day 10), or two and two (day 20) in Cre-Ad group and Smad7-Ad group, respectively. The efficiency of gene transfer was evaluated by co-infection of Cre-Ad and GFP (green fluorescein protein) under control of the Cre/LoxP system. Expression of GFP was evaluated in unfixed cryosections using fluorescent microscopy.

### *Alkali Burn in Smad3-Knockout Mice*

To compare the effects of *Smad7* gene transfer and loss of *Smad3* on the healing process after alkali burn in a cornea, a similar alkali burn was administered to corneas of Smad3 knockout mice (a mixture of three strains; C57BL/6/NIH Swiss/SV129). Twenty-four eyes total of 12 Smad3<sup>+/+</sup> mice and 12 Smad3<sup>-/-</sup> mice were examined at days 5, 10, or 20 after alkali burn. The enucleated eyes were processed for paraffin sections as described above. For assay of expression of mRNAs of cytokines, real-time reverse transcriptase (RT)-polymerase chain reaction (PCR) was performed as described above. Alkali-burned corneas of Smad3<sup>+/+</sup> and Smad3<sup>-/-</sup> mice were obtained at days 10 and 20 after burn ( $n = 4$  at each time point) and processed for tRNA extraction and real-time RT-PCR as described below. Four uninjured corneas of two Smad3<sup>+/+</sup> mice and six of three Smad3<sup>-/-</sup> mice were included to obtain the basal expression level of each cytokine.

### *Immunohistochemistry*

Deparaffinized sections (5  $\mu$ m thick) or cryosections (7  $\mu$ m thick) fixed in cold acetone for 5 minutes were processed for indirect immunohistochemistry. The following antibodies were used; rabbit polyclonal anti-Smad3 antibody [(1:100 dilution in phosphate-buffered saline (PBS); Zymed, South San Francisco, CA)], goat polyclonal anti-Smad7 antibody (1:300 in PBS; Santa Cruz Biotechnology, Santa Cruz, CA), rabbit polyclonal anti-phosphorylated p65/RelA of NF- $\kappa$ B (1:50 dilution in PBS; Cell Signaling, Beverly, MA), rabbit polyclonal anti-keratin 12 antibody (1  $\mu$ g/ml in PBS), mouse monoclonal anti- $\alpha$ -SMA antibody (1:100 dilution in PBS; Neomarker, Fremont, CA), rat monoclonal anti-laminin antibody (1:25 dilution in PBS; Sigma, St. Louis, MO), goat polyclonal anti-MCP-1 (1:100 dilution in PBS, Santa Cruz), goat polyclonal anti-connective tissue growth factor (CTGF) antibody (1:100 dilution in PBS, Santa Cruz), goat polyclonal anti-VEGF (1:100 dilution in PBS, Santa Cruz), goat polyclonal anti-type IV collagen antibody (1:100 in PBS; Southern Biotechnology, Birmingham AL), and rat monoclonal anti-CD31 (PECAM) antibody (1:100 in PBS, Santa Cruz). The rat monoclonal F4/80 anti-macrophage antigen antibody (clone A3-1, 1:400 dilution in PBS; BMA Biomedicals, Augst, Switzerland) was used to detect monocytes/macrophages. The number of labeled cells in the central cornea (200  $\mu$ m in length) was determined in four corneas in each treatment group. Fluorescein isothiocyanate-conjugated specific secondary antibodies were used for detection of the primary antibody and 4,6-diamidino-2-phenylindole (DAPI) was used for nuclear counterstaining. Cell proliferation in the healing epithelium was determined by immunostaining with an anti-BrdU antibody (1:11 in PBS; Roche

Diagnosics, Mannheim, Germany) and diaminobenzidine reaction with hematoxylin counterstaining as previously reported<sup>53</sup> followed by counting the number of labeled cells in healing epithelia in the affected cornea. Specimens were treated with 2 N HCl for 60 minutes at 37°C before antibody application. Immunohistochemistry for TGF- $\beta$ s was performed as previously reported.<sup>54,55</sup>

### *Expression of mRNAs of TGF- $\beta$ 1, TGF- $\beta$ 2, MCP-1, VEGF, MMP-2, MMP-9, Smad7, and Tissue Inhibitors of Metalloproteinases (TIMP)-1 and -2 in Burned Corneas by Using Real-Time RT-PCR*

For extraction of RNA, alkali-burned corneas from seven mice were obtained from each treatment group [C57BL/6 mice ( $n = 28$ ), Smad3<sup>+/+</sup> mice ( $n = 8$ ), or Smad3<sup>-/-</sup> mice ( $n = 8$ )] at days 10 or 20 and stored at -80°C. Untreated corneas of three C57BL/6 mice, two Smad3<sup>+/+</sup> mice, and six Smad3<sup>-/-</sup> mice were also included to get the baseline mRNA expression. Total RNA from corneal tissue excised from a burned eye was extracted using ISO GENE (Nippon Gene, Tokyo, Japan) according to the manufacturer's protocol and processed for semiquantitative real-time RT-PCR for mRNAs of mouse *TGF- $\beta$ 1*, *TGF- $\beta$ 2*, *mcp-1*, *vegf*, *Smad7*, *mmp-9*, and *timp-2*. For the real-time RT-PCR, the TaqMan one-step RT-PCR master mix reagents kit and the Applied Biosystems Prism 7700 (PE Applied Biosystems, Foster City, CA) were used as previously described. Primers and oligonucleotide probes were designed according to the cDNA sequences in the GenBank database using the Primers Express software (PE Applied Biosystems) and are listed in Table 1. RT-PCR conditions were as follows: 2 minutes at 50°C (stage 1, reverse transcription), 10 minutes at 95°C (stage 2, reverse transcription inactivation and AmpliTaq Gold activation), and then 40 cycles of amplification for 15 seconds at 95°C and 1 minute at 60°C (stage 3, PCR).

**View this table:** [Table 1. Primers and Oligonucleotide Probes](#)  
[\[in this window\]](#)  
[\[in a new window\]](#)

### *Effect of Exogenous Smad7 on NF- $\kappa$ B Signaling in Cultured Cells*

Simian virus (SV)-40 large T-antigen-immortalized human corneal epithelial cells (Araki-Sasaki cells)<sup>56</sup> provided by the Riken Cell Bank (Tokyo, Japan) were used to examine the effect of overexpression of exogenous Smad7 on NF- $\kappa$ B signaling. The cells ( $2.0 \times 10^5$ /six-well culture plate or  $2.0 \times 10^4$ /16-well chamber slides; Nalge Nunc Int., Naperville, IL) were cultured in Dulbecco's modified Eagle's medium/F-12 mixture medium supplemented with 10% fetal bovine serum, 5  $\mu$ g/ml cholera toxin, 5 mg/ml insulin, 10 ng/ml human epidermal growth factor, and antibiotics for 24 hours until confluent. Cells were then incubated for 2 hours in a serum-free medium containing Cre-Ad or both Cre-Ad and Smad7-Ad at a concentration of  $4 \times 10^3$  PFU/ml, and then incubated for another 48 hours in Dulbecco's modified Eagle's medium/F-12 medium supplemented with 10% fetal bovine serum, 5  $\mu$ g/ml cholera toxin, and antibiotics. Cells were then exposed to 10 ng/ml of recombinant human tumor necrosis factor (TNF)- $\alpha$  (R&D Systems, Minneapolis, MN) for 30 minutes, 1 hour, and 2 hours and were processed for



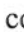
immunocytochemistry and Western blotting.

For Western blotting, cells in six-well plates were homogenized in a lysis buffer (100 ml of CelLytic-M mammalian cell lysis/extraction reagent; Sigma) supplemented with a cocktail of proteinase inhibitors (Complete protease inhibitor cocktail tablet; Rosch, Mannheim, Germany). The cell lysate was centrifuged, mixed with 3X sample buffer, run on sodium dodecyl sulfate-polyacrylamide gel electrophoresis, transferred to polyvinylidene difluoride membrane, and Western blotted for Smad7 (Santa Cruz), total RelA (Santa Cruz), phospho-RelA (Cell Signaling), and  $\beta$ -actin (Santa Cruz). Phospho-RelA was determined on polyvinylidene difluoride membranes first stained for total RelA and stripped. To determine nuclear proteins, cells were fractionated into cytoplasm and nuclei by using ProteoExtract subcellular proteome extraction kit (Calbiochem, Darmstadt, Germany) according to the manufacturer's protocol and processed as above. Immunoreactive bands were visualized on Lumino analyzer LAS1000 (Fujifilm, Tokyo, Japan), using enhanced chemiluminescence Western blotting detection reagents (Amersham Bioscience, Piscataway, NJ). For immunocytochemistry, cells in Nunc 16-well chamber slides were immunostained with antibody against Smad7, total RelA, or phospho-RelA and detected as above.

## ► Results

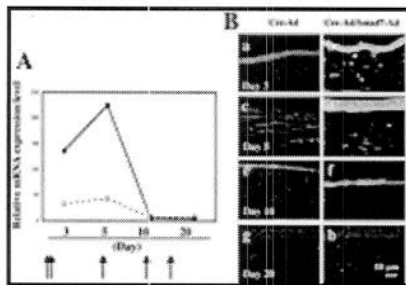
### *Efficiency of Adenoviral Gene Transfer into a Burned Mouse Cornea*

The efficiency of gene transfer was evaluated by co-infection of adenoviruses carrying Cre under control of the CAG promoter and GFP under control of the Cre/LoxP system. Our preliminary experiments in uninjured mouse corneas or corneas with a central epithelial 2-mm debridement showed that although adenovirus infected conjunctival epithelium efficiently, it infected corneal epithelium only weakly, and did not infect keratocytes in agreement with previously published studies.<sup>57</sup> In contrast, in the total ocular surface alkali burn model used in the present study, we administered the GFP-expressing adenovirus at 2 and 24 hours and day 5 and the cryosections of day 5 or day 10 specimens were observed under fluorescence microscope without fixation. GFP expression was easily detected in conjunctival epithelium, subconjunctival fibroblasts, keratocytes, and healing epithelium at day 5 and very weakly in epithelium at day 10 (data not shown).

A mixture of Cre-Ad and a recombinant adenovirus carrying mouse *Smad7* cDNA under control of the Cre/LoxP system was administered at 2 and 24 hours, and days 5, 10, and 15 after an alkali exposure (hereafter referred to as Smad7-Ad). Cre recombinase expressed via the CAG promoter deletes the stuffer PolyA through the Cre/LoxP system, leading to expression of Smad7. Real-time RT-PCR showed up-regulation of Smad7 mRNA at days 3 and 5 in both Cre-Ad and Smad7-Ad groups (Figure 1a) , with expression levels being much higher in Smad7-Ad group as compared with Cre-Ad group at these time points. In both groups Smad7 mRNA expression rapidly declined at day 10 (Figure 1A) , suggesting that administration of Smad7-Ad to the healing cornea at days 10 and 15 had no effect, consistent with the nearly complete extent of healing at this time point (Figure 2A) .

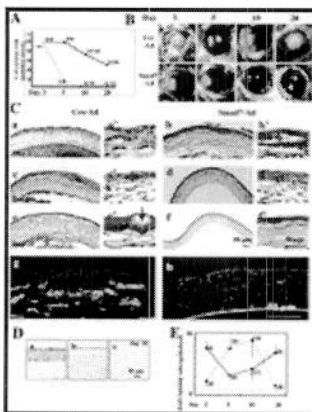
- |   |
|---|
| ▲ <a href="#">Top</a>                   |
| ▲ <a href="#">Abstract</a>              |
| ▲ <a href="#">Materials and Methods</a> |
| ▪ <a href="#">Results</a>               |
| ▼ <a href="#">Discussion</a>            |
| ▼ <a href="#">References</a>            |

Immunohistochemical analysis showed that almost no Smad7 was detected in uninjured corneal epithelium and keratocytes (or corneal fibroblasts) (data not shown). At days 3 to 5 a faint immunoreactivity for endogenous Smad7 was detected in healing epithelium or keratocytes in corneas of the Cre-Ad control group (Figure 1B, a and c) [1]. On the other hand, marked expression of exogenous Smad7 was seen in healing epithelium on the burned cornea and keratocytes in the Smad7-Ad group (Figure 1B, b and d) [1]. At day 10, weak Smad7 staining was still detected in the regenerated epithelium in the Smad7-Ad-treated cornea (Figure 1B, f) [1], but it was still more intense than that in a Cre-Ad group cornea (Figure 1B, e) [1]. Smad7 was barely detectable at day 20 in both groups (Figure 1B, g and h) [1], consistent with the RT-PCR results.



**View larger version (33K):**  
[\[in this window\]](#)  
[\[in a new window\]](#)

**Figure 1.** Detection of adenovirally introduced Smad7 in the healing mouse cornea after alkali burn. **A:** Real-time RT-PCR showed a marked up-regulation of Smad7 mRNA at days 3 and 5 after injury in Smad7-Ad groups, compared to the Cre-Ad group. In both groups levels of Smad7 mRNA were strongly reduced at day 10. Corneas were treated topically with Smad7-Ad at 2 and 24 hours, and again at days 5, 10, and 15 as indicated. Data represent a typical result in one experiment of four done at each time point. **Arrows** indicate the points of viral vector administration. **B:** Immunohistochemical analysis showed that a faint immunoreactivity for endogenous Smad7 was detected in healing epithelium or keratocytes in corneas of the Cre-Ad control group at days 3 to 5 (**a, c**). On the other hand, marked expression of exogenous Smad7 was seen in healing epithelium and keratocytes in the Smad7-Ad group (**b, d**). At day 10, weak Smad7 staining was still detected in the regenerated epithelium in the Smad7-Ad-treated cornea (**f**), but it was more intense than that in a Cre-Ad group cornea (**e**). It was then barely detectable at day 20 in both groups (**g, h**), Nuclei are counterstained with DAPI. Scale bar, 10  $\mu$ m.



**View larger version (71K):**

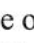
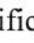
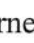
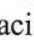
**Figure 2.** Healing of an alkali-burned mouse cornea treated with either Smad7-Ad or Cre-Ad. **A:** Scoring of the percent incidence of corneas of C57BL/6 mice with an epithelial defect at each time point in Cre-Ad (**solid line**) or Smad7-Ad-treated (**dotted line**) groups. At day 10 all of the corneas in the Smad7-Ad group were re-epithelialized, whereas at day 20, 50% of the corneas in the Cre-Ad group still showed defects. **B:** Macroscopic observation of the corneal defects as visualized by staining with fluorescein to allow visualization of cornea defects in green shows the extent of the ocular surface burn in the Cre-Ad- (**a**) and Smad7-Ad-treated (**e**) groups at day 3. In the Cre-Ad group, epithelial defects with stromal opacification are observed at days 5 (**b**) and 10 (**c**), with re-epithelialization and dense stromal opacification at day 20 (**d**). Defects seen in corneas treated with Smad7-Ad were typically






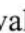

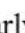



[in this window]  
[in a new window]


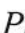
smaller at day 5 (**f**) and the cornea is almost transparent at days 10 (**g**) and 20 (**h**). **C:** Histology of burned corneas stained with H&E. No histological differences were seen in the central corneas of the Cre-Ad group (**a**, **a'**) and Smad7-Ad group (**b**, **b'**) at day 3. Bleeding and inflammation in the anterior chamber are more marked in the Cre-Ad group as compared with the Smad7-Ad group. Higher magnification pictures show the majority of cells in the burned stroma to be inflammatory cells (**a'**, **b'**). At day 10 Cre-Ad-treated corneas often show epithelial in-growth into the stroma (**asterisk**, **c**, **c'**), whereas Smad7-Ad-treated corneas exhibit a regenerated epithelium with nearly normal stratification (**epi**) (**d**, **d'**). At day 20 corneas in the Cre-Ad group still show a significant hypercellularity (presumed to be both inflammatory cells and corneal stromal cells), conjunctivalization of resurfaced epithelium and thicker stroma (**e**, **e'**), whereas corneas in the Smad7-Ad group exhibit a well-regenerated epithelium with a less cellularity in the stroma (**f**, **f'**). Higher magnification pictures show the presence of many goblet cells (**arrows**) in conjunctival epithelium resurfacing a Cre-Ad-treated cornea (**e'**), whereas the epithelium in a Smad7-Ad-treated cornea exhibits a cornea-like morphology (**f'**). Immunofluorescence staining for type IV collagen shows a disrupted basement membrane and ectopic type IV collagen deposition in the stroma in a Cre-Ad-treated cornea at day 20 (**g**), whereas the basement membrane remains intact in a Smad7-Ad-treated cornea (**h**). **epi**, healing epithelium. Nuclei are counterstained with DAPI in **g** and **h**. **D:** Whereas the uninjured mouse cornea stains positively for keratin 12 (**a**), regenerated epithelium in burned corneas is conjunctiva-derived and keratin 12-negative in both a Cre-Ad cornea (**b**) and a Smad7-Ad-treated cornea (**c**) at day 10 after injury. **E:** Cell proliferation in either Cre-Ad-treated (**dotted line**) or Smad7-Ad-treated (**solid line**) corneas at days 3 to 20 after injury as detected by BrdU incorporation. Bar, SD of the number (in parentheses) of corneas examined. Scale bars: 50  $\mu$ m (**C**); 10  $\mu$ m (**D**).

### *Alkali-Burned Corneas Treated with Adenoviral Gene Transfer of Smad7 Show Improved Healing*

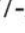


Because preliminary experiments showed no obvious differences in either the histology or the rate of healing of alkali-burned mouse corneas treated with either Cre-Ad alone or no vector, we used corneas of the Cre-Ad group as controls. Green fluorescein staining was used to evaluate healing of the corneal surface as quantitated by the presence or absence of an epithelial defect/ulceration (Figure 2A) , and the degree of macroscopic corneal stromal opacification (Figure 2B) . At day 10 after injury, 13 of 18 corneas of the Cre-Ad group still showed an epithelial defect or stromal ulceration, whereas 0 of 20 corneas treated with Smad7-Ad showed any defects. At this same time point, corneas in the Cre-Ad group that remained free of epithelial defects (5 of 18) exhibited dense stromal opacification, compared to minimal stromal opacification in all of the corneas of Smad7 group (Figure 2B, c versus g) . At day 20 after injury, 50% of the corneas in the Cre-Ad group still exhibited epithelial defects/ulceration and the remaining corneas showed dense stromal opacification (Figure 2B, d) . In contrast, all corneas in

the Smad7-Ad group exhibited only minor opacification without epithelial defects (Figure 2B, h)  .


Hematoxylin and eosin (H&E) staining (Figure 2C)  showed that although burned corneas of both Cre-Ad and Smad7-Ad groups showed epithelial defects and stromal inflammation at day 3 (Figure 2C; a, a', b, b')  , at day 10, corneas in the Cre-Ad group were characterized by a less organized epithelium with invasion into the underlying stroma (Figure 2C; c, c', d, d')  . The absence of staining for keratin 12, which is expressed in corneal, but not conjunctival epithelium (see uninjured cornea in Figure 2D, a)  , showed that the regenerated epithelium in both Cre-Ad- (Figure 2D, b)  and Smad7-Ad-treated groups (Figure 2D, c)  was of conjunctival origin, regardless of the more organized appearance in the Smad7-Ad-treated eyes. At day 20, corneas in the Cre-Ad group were, on average, thicker than corneas in the Smad7-Ad group, which had remodeled to a nearly normal thickness (Figure 2C; e, e', f, f')  . Importantly, the conjunctival epithelium resurfacing the corneas in the Smad7-Ad group transdifferentiated into cornea-like epithelium, while that resurfacing the healing corneas in the Cre-Ad group showed conjunctivalization (Figure 2C, e' versus f')  , as indicated by the presence of many mucin-secreting goblet cells (arrows).

Development of corneal ulceration after alkali burn is characterized by degradation of the epithelial basement membrane by MMPs expressed by healing epithelial cells and keratocytes as well as by inflammatory cells. Immunostaining of healing corneas in the Cre-Ad control group for type IV collagen, showed disruption of the basement membrane and loss of epithelial integrity beginning at day 5 (data not shown) and continuing through day 20 (Figure 2C, g)  . In contrast, corneas in the Smad7-Ad group showed a linear pattern of subepithelial immunoreactivity indicating an intact basement membrane (Figure 2C, h)  .

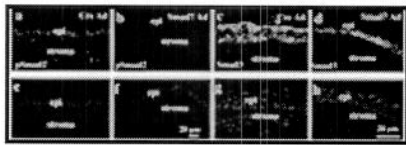
### *Smad7 Expression Alters the Proliferative Profile of the Healing Epithelium*

Proliferation and migration of regenerated epithelium are critical to corneal healing after alkali injury, and both are known to be responsive to TGF- $\beta$ /Smad signaling. Such epithelial cell proliferation is considered to be modulated in a complex way by both autocrine and paracrine signaling. Quantitation of BrdU staining showed that treatment with Smad7-Ad (solid line, Figure 2E)  ) profoundly alters the time course of proliferation of conjunctival epithelium, enhancing proliferation at early times after injury but suppressing it from days 5 to 10 after injury, compared to Cre-Ad-treated eyes (dotted line, Figure 2E)  . At the latest time point, day 20 after injury, epithelial proliferation in the Smad7-Ad group was again enhanced compared to controls (Figure 2E)  .

### *Smad Signaling in the Injured Cornea Is Inhibited by Exogenous Smad7*

To investigate whether treatment with Smad7-Ad blocks Smad signaling in alkali-burned corneas, specimens were immunostained with antibodies against phosphorylated Smad2, as an indicator of activation of Smad signaling. At day 5 after injury, when expression of exogenous Smad7 was high, phospho-Smad2 was detected in the nuclei of healing epithelium and keratocytes in the Cre-Ad-treated group, but to a greatly reduced extent in eyes treated with Smad7-Ad (Figure 3, a versus b)  . Similarly, at day 5 after burn, Smad3 was detected in the cytoplasm and nuclei of many epithelial cells in Cre-Ad

group cornea, whereas it mainly localized to the cytoplasm of epithelial cells in Smad7-Ad group (Figure 3, c versus d) [17].

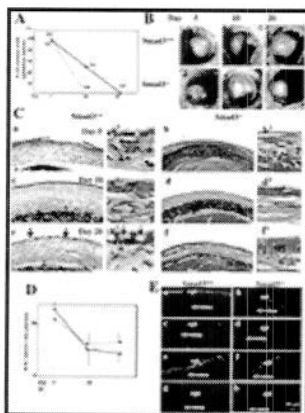


**View larger version (23K):**  
[\[in this window\]](#)  
[\[in a new window\]](#)

**Figure 3.** Smad signaling status in alkali-burned corneas treated with Cre-Ad or Smad7-Ad at day 5. At day 5 after injury, staining for nuclear phospho-Smad2 is detected in the healing epithelium and stromal cells in the peripheral cornea treated with Cre-Ad (**a**), whereas it is not seen in the healing epithelium and stromal cells of a Smad7-Ad-treated cornea (**b**). Smad3 is detected in the cytoplasm and nuclei of the healing epithelium and faintly in stromal cells in a cornea treated with Cre-Ad (**c**), whereas Smad3 is located mainly in the cytoplasm of healing epithelium and stromal cells in the Smad7-Ad group (**d**). **e to h**: The nuclei of **a to d** as visualized by DAPI staining. epi, epithelium. Scale bars, 20  $\mu$ m.

### Effect of Loss of Smad3 on Corneal Healing

Because Smad2/3 signaling is known to be inhibited by Smad7<sup>41,42</sup> and because we have previously shown enhanced healing of an incisional skin wound in mice in which Smad3 has been deleted,<sup>17</sup> we evaluated healing of corneas of Smad3-knockout mice after alkali burn. Throughout the time period of observation, the degree of tissue damage and inflammation from the alkali injury was less severe in the mixed C57BL/6/NIH Swiss/SV129 genetic background of the Smad3<sup>+/+</sup> mice, compared to that of the C57BL/6 mice used for the adenoviral study, with or without viral vector application. Although corneas from Smad3<sup>-/-</sup> mice showed a lesser incidence of epithelial defects and stromal thickening at day 10 than Smad3<sup>+/+</sup> controls (Figure 4A) [17], corneas of both Smad3<sup>+/+</sup> and Smad3<sup>-/-</sup> were free from ulceration [Figure 4, A and B (b, e) [17]]. However, at day 20, corneas from both Smad3<sup>+/+</sup> and Smad3<sup>-/-</sup> mice remained opaque (Figure 4B, c and f) [17], in contrast to those C57BL/6 mice treated with Smad7-Ad, which were almost transparent at this time point (Figure 2B, h) [17].












**View larger version (69K):**

**Figure 4.** Healing of alkali-burned corneas of Smad3-knockout mice. **A**: The percent incidence of corneas with an epithelial defect at each time point in Smad3<sup>+/+</sup> ( $n = 4$ , **solid line**) and Smad3<sup>-/-</sup> ( $n = 4$ , **dotted line**) mice. Epithelial resurfacing is accelerated in Smad3<sup>-/-</sup> mice. **B**: Macroscopic observation shows total ocular surface burn in both Smad3<sup>+/+</sup> (**a**) and Smad3<sup>-/-</sup> (**d**) mice at day 5. At day 10, an epithelial defect with stromal opacification is observed in a Smad3<sup>+/+</sup> cornea (**b**), whereas the burned cornea has been resurfaced in Smad3<sup>-/-</sup> (**e**) mice. Although all of the corneas in both Smad3<sup>+/+</sup> (**c**) and Smad3<sup>-/-</sup> (**f**) mice have been resurfaced by day 20, stromal opacification is more marked in Smad3<sup>+/+</sup> mice. **C**: Histology of burned corneas of Smad3-knockout mice stained with H&E. An

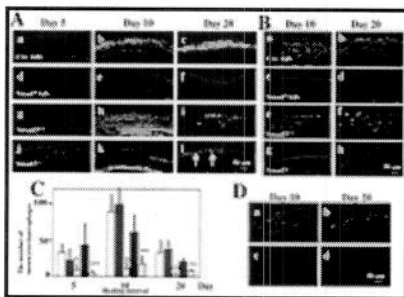
[in this window]  
[in a new window]

epithelial defect is observed in both Smad3<sup>+/+</sup> (**a, a'**) and Smad3<sup>-/-</sup> (**b, b'**) mice at day 5. The burned stroma is thinner in a Smad3<sup>-/-</sup> mouse (**b, b'**) as compared with that in a Smad3<sup>+/+</sup> mouse (**a, a'**). Higher magnification pictures (**a', b'**) suggest that the majority of cells in the burned stroma are inflammatory cells at day 5. At day 10 the burned corneas in both Smad3<sup>+/+</sup> and Smad3<sup>-/-</sup> mice have been resurfaced (**c, c', d, d'**) and stroma is again thinner in a Smad3<sup>-/-</sup> mouse (**c** versus **d**). At day 20, the corneal surface is covered with conjunctival epithelium with abundant goblet cells in a Smad3<sup>+/+</sup> mouse (**e** and **e', arrows**), whereas the epithelium in Smad3<sup>-/-</sup> mice is cornea-like (**f, f'**). The thickened stroma of a Smad3<sup>+/+</sup> mouse compared to that of a Smad3<sup>-/-</sup> mouse persists at this time point. **D:** Cell proliferation in healing corneas as detected by BrdU incorporation. There is no difference of the number of BrdU-labeled epithelial cells between Smad3<sup>+/+</sup> mice (**solid line**) and Smad3<sup>-/-</sup> mice (**dotted line**) at each healing interval. Bar, SD. **E:** Immunofluorescent staining for phospho-Smad2 (**a, b, e, f**) in the central (**a to d**) or peripheral (**e to h**) corneas of Smad3<sup>+/+</sup> (**a, c, e, g**) and Smad3<sup>-/-</sup> (**b, d, f, h**) mice at day 10 after alkali burn. Nuclear staining for phospho-Smad2 is more marked in the healing corneal epithelium (epi) of Smad3<sup>+/+</sup> mice than in Smad3<sup>-/-</sup> mice. **c, d, g, and h:** DAPI nuclear staining of the area seen in **a, b, e, and f**, respectively. Scale bars: 20  $\mu\text{m}$  (**E**); 50  $\mu\text{m}$  (**C**).

Examination of the histology of healing corneas of Smad3<sup>-/-</sup> mice confirmed accelerated healing compared to eyes of Smad3<sup>+/+</sup> littermates (Figure 4C) . Stromal edema and infiltration of inflammatory cells were more prominent in Smad3<sup>+/+</sup> mice (Figure 4C; **a, a', c, c', e, e'**)  than in Smad3<sup>-/-</sup> littermates (Figure 4C; **b, b', d, d', f, f'**)  at each time point examined. Even though these mice showed less severe injury than the C57BL/6 mice, at day 20, healed corneas in Smad3<sup>-/-</sup> mice still exhibited a thickened edematous, less-organized, stroma (Figure 4C, **f**) , as compared with burned corneas of C57BL/6 mice treated with Smad7-Ad (Figure 2C, **f**) . As in both the Smad7-Ad and Cre-Ad-treated groups of C57BL/6 mice, the resurfacing epithelium of Smad3-knockout mice was negative for keratin 12 regardless of the Smad3 genotype (data not shown). Also consistent with the Smad7-Ad treated corneas, regenerated epithelia in Smad3<sup>+/+</sup> mice exhibited a conjunctival phenotype as evidenced by the presence of many goblet cells (arrows), whereas that in Smad3<sup>-/-</sup> mice lacked goblet cells at day 20 (Figure 4C, **e** and **f**) . In contrast to the effects seen with Smad7-Ad treatment of C57BL/6 mice, epithelial cell proliferation as evaluated by BrdU incorporation was not affected by the Smad3 genotype (Figure 4D) . Assessment of the effects of loss of Smad3 on Smad2 signaling in the healing cornea showed markedly less staining for phospho-Smad2 in both the central (Figure 4E, **a** and **b**)  and peripheral cornea of Smad3<sup>-/-</sup> mice compared to Smad3<sup>+/+</sup> littermates day 10 after injury (Figure 4E, **e** and **f**) .

### *Formation of Myofibroblasts Is Associated with the Poorer Healing in Cre-Ad and Smad3<sup>+/+</sup> Corneas*

One of the hallmarks of scar tissue formation and opacification of corneal stroma is the well-established transdifferentiation of keratocytes into  $\alpha$ -SMA-positive myofibroblasts.<sup>58-61</sup> Examination of the expression pattern of  $\alpha$ -SMA in injured corneas showed that, at day 10 after injury, many stromal cells in injured corneas of Cre-Ad-treated mice and Smad3<sup>+/+</sup> mice expressed  $\alpha$ -SMA (Figure 5A, b and h), respectively), but that this was substantially reduced in Smad7-Ad-treated and Smad3<sup>-/-</sup> mice (Figure 5A, e and k), respectively). Although these differences persisted at day 20 after wounding (Figure 5A; c, f, i, and l), it is important to note that  $\alpha$ -SMA staining was still detectable (arrows in Figure 5A, l) in corneas of Smad3<sup>-/-</sup> mice at this time point, whereas it was below the level of detection in corneas treated with Smad7-Ad (Figure 5A, f), consistent with the better outcome in that group.

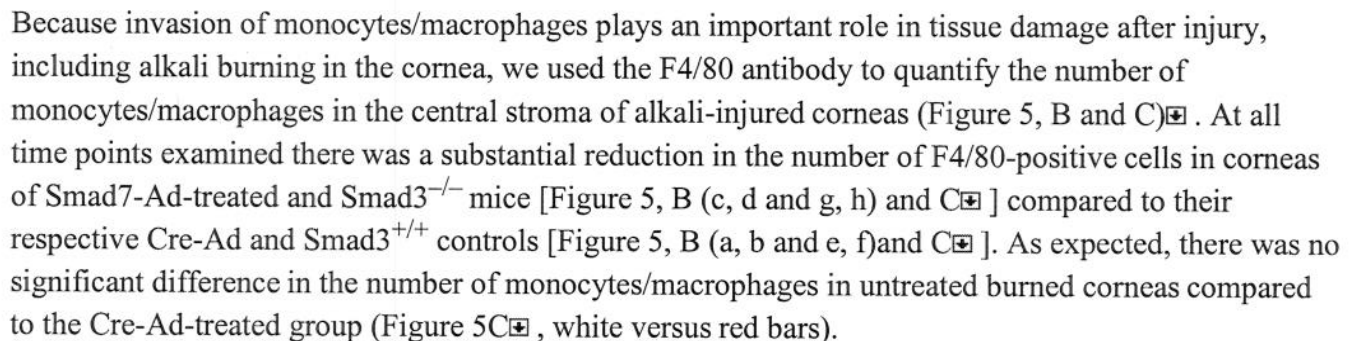
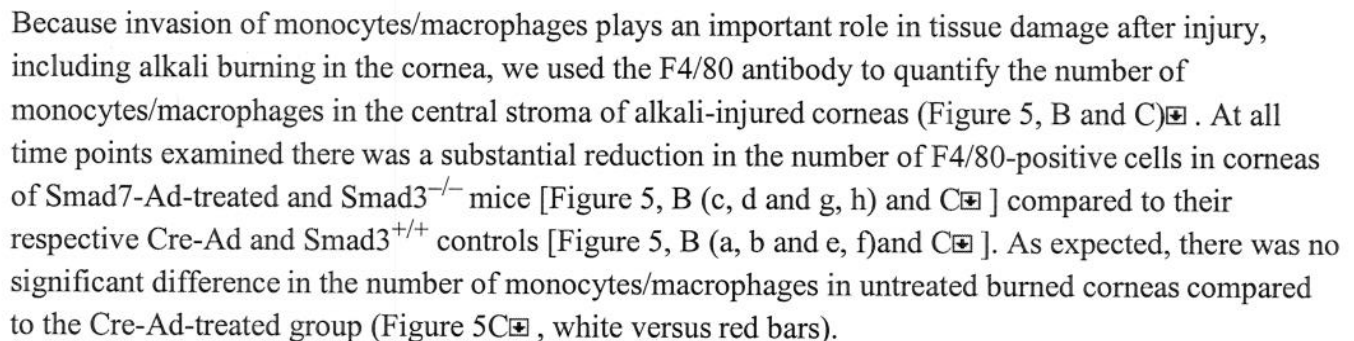
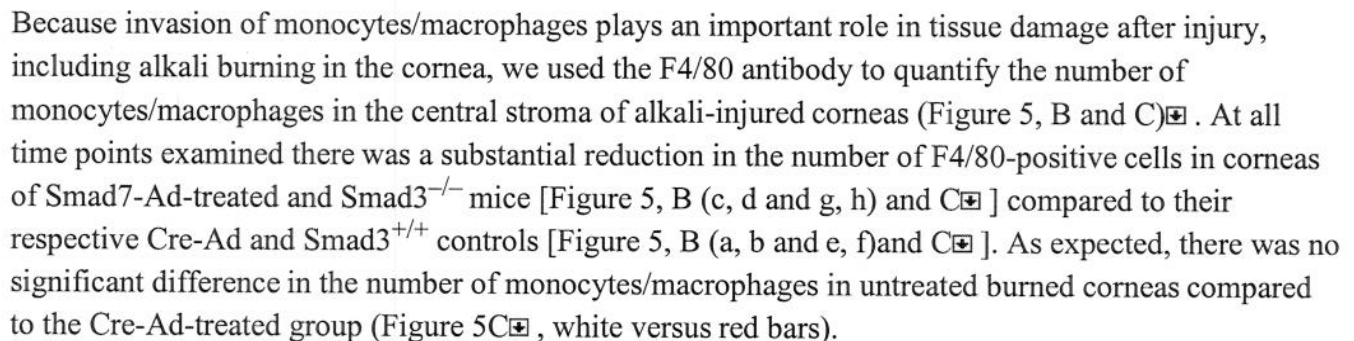
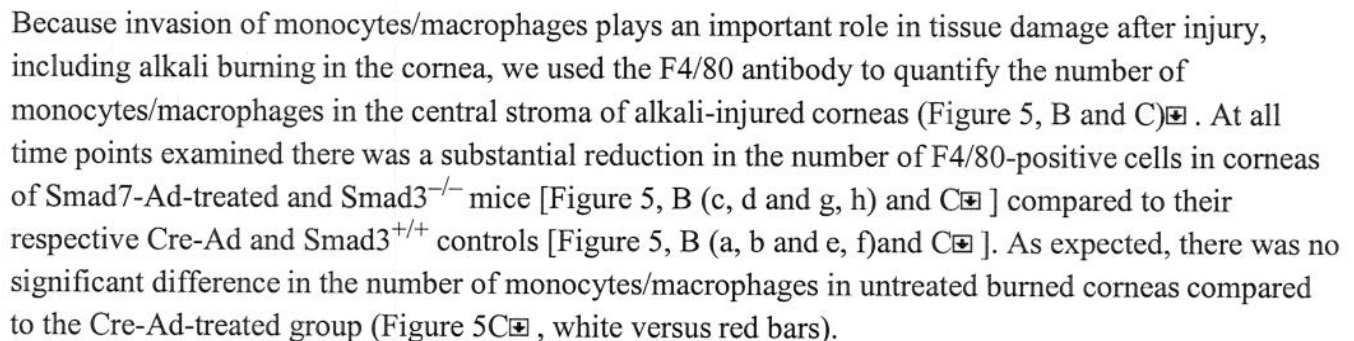


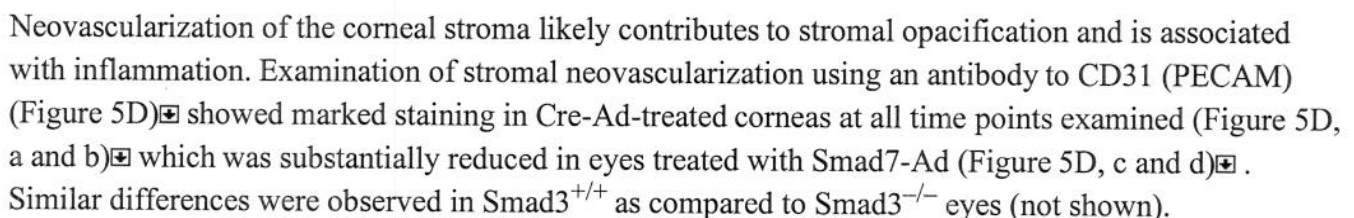
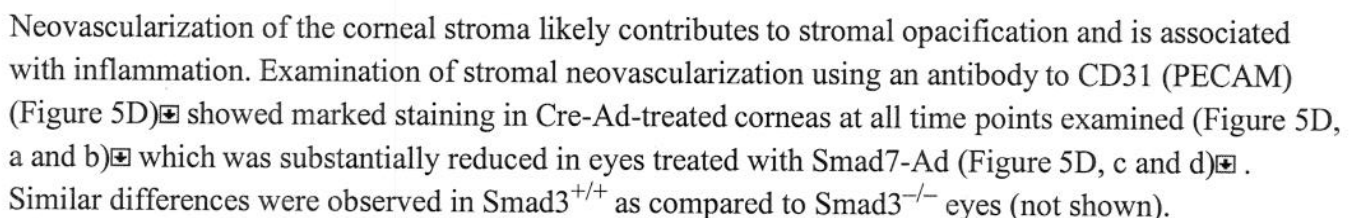
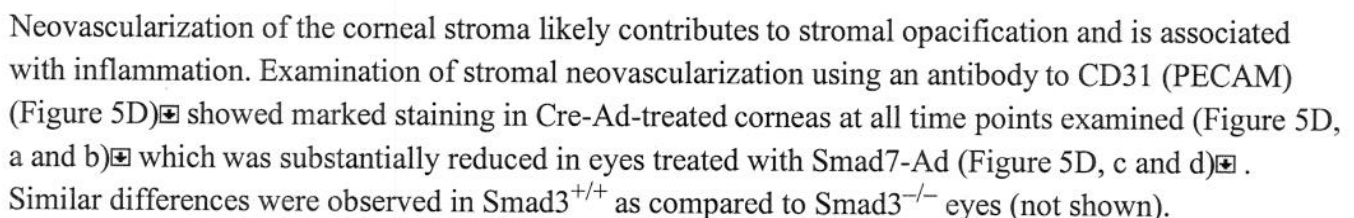
**View larger version (58K):**  
[\[in this window\]](#)  
[\[in a new window\]](#)

**Figure 5.** Analysis of stromal healing in burned corneas. **A:** The expression pattern of  $\alpha$ -smooth muscle actin ( $\alpha$ -SMA) as detected by immunofluorescence in stromal cells at days 5 (**a, d, g, j**), 10 (**b, e, h, k**), and 20 (**c, f, i, l**) after alkali burn of either Cre-Ad (**a to c**) or Smad7-Ad-treated (**d to f**) C57BL/6 mice. The same analysis was done in Smad3<sup>+/+</sup> (**g to i**) and Smad3<sup>-/-</sup> (**j to l**) mice. At day 5 no  $\alpha$ -SMA-positive cells are observed in the burned stroma of corneas treated with either Cre-Ad (**a**) or Smad7-Ad (**d**). In burned corneas treated with Cre-Ad, stromal cells expressing  $\alpha$ -SMA are observed at days 10 (**b**) and 20 (**c**), whereas such cells are seen only occasionally at day 10 (**e**) and are absent at day 20 (**f**) in corneas treated with Smad7-Ad. In Smad3<sup>+/+</sup> mice (**g to i**) and Smad3<sup>-/-</sup> mice (**j to l**) stromal cells expressing  $\alpha$ -SMA are observed throughout the healing interval up to day 20 with a peak at day 10 (**h, k**). However,  $\alpha$ -SMA expression is more marked in Smad3<sup>+/+</sup> mice (**h, i**) as compared with that in Smad3<sup>-/-</sup> mice (**k, l**) at both days 10 (**h, k**) and 20 (**i, l**). **B:** The presence and distribution of F4/80-positive monocytes/macrophages as detected by immunofluorescence in representative areas of the burned corneal stroma at days 10 (**a, c, e, g**) and 20 (**b, d, f, h**) in either Cre-Ad (**a, b**) or Smad7-Ad-treated (**c, d**) C57BL/6 mice or in Smad3<sup>+/+</sup> (**e, f**) and Smad3<sup>-/-</sup> mice (**g, h**). Labeled cells (monocytes/macrophages) are distributed throughout the stroma in corneas treated with Cre-Ad (**a, b**), whereas a few, if any, labeled cells are seen in the stroma of corneas treated with Smad7-Ad (**c, d**) at days 10 (**a, c**) and 20 (**b, d**). Similarly, the burned stromas of Smad3<sup>+/+</sup> mice show many monocytes/macrophages at days 10 (**e**) and 20 (**f**), whereas many fewer cells are detected in the Smad3<sup>-/-</sup> mice (**g, h**). **C:** Bar graph of the number of monocytes/macrophages in the central stroma at days 5 to 20 after injury determined as described in Materials and Methods: C57BL/6 mice untreated (**white bar**), treated with Cre-Ad (**red bar**), or treated with

Smad7-Ad (**pink bar**); Smad3<sup>+/+</sup> mice (**dark blue bar**), Smad3<sup>-/-</sup> mice (**light blue bar**). The number of monocytes/macrophages in the stroma of corneas treated with Smad7-Ad is significantly reduced compared to that of corneas treated with Cre-ad at all time points examined. Whereas levels of monocytes/macrophages in Smad3<sup>+/+</sup> mice is less than in C57BL/6 mice at days 10 and 20 (**dark blue bar**), loss of Smad3 in the mice of this background further reduces the number of such cells at all time points (**light blue bar**). \*\* or \*\*\* indicate  $P < 0.05$  or  $P < 0.01$ , respectively, for comparisons of Smad7-Ad against Cre-Ad and of Smad3<sup>-/-</sup> against Smad3<sup>+/+</sup> data. **D**: Stromal neovascularization after alkali burn as detected by immunofluorescent staining using an antibody against PECAM (CD31). At each time point, stromal neovascularization was suppressed by application of Smad7-Ad vector (**c, d**) as compared with Cre-Ad (**a, b**). Nuclei are counterstained with DAPI in **A, B**, and **D**. Scale bars, 50  $\mu\text{m}$ .

### *Smad7-Ad-Treated and Smad3<sup>-/-</sup> Corneas Exhibit Less Damage to the Stromal Compartment*

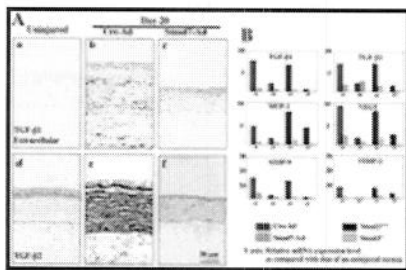
Because invasion of monocytes/macrophages plays an important role in tissue damage after injury, including alkali burning in the cornea, we used the F4/80 antibody to quantify the number of monocytes/macrophages in the central stroma of alkali-injured corneas (Figure 5, B and C) . At all time points examined there was a substantial reduction in the number of F4/80-positive cells in corneas of Smad7-Ad-treated and Smad3<sup>-/-</sup> mice [Figure 5, B (c, d and g, h) and C ] compared to their respective Cre-Ad and Smad3<sup>+/+</sup> controls [Figure 5, B (a, b and e, f) and C ]. As expected, there was no significant difference in the number of monocytes/macrophages in untreated burned corneas compared to the Cre-Ad-treated group (Figure 5C , white versus red bars).

Neovascularization of the corneal stroma likely contributes to stromal opacification and is associated with inflammation. Examination of stromal neovascularization using an antibody to CD31 (PECAM) (Figure 5D)  showed marked staining in Cre-Ad-treated corneas at all time points examined (Figure 5D, a and b)  which was substantially reduced in eyes treated with Smad7-Ad (Figure 5D, c and d) . Similar differences were observed in Smad3<sup>+/+</sup> as compared to Smad3<sup>-/-</sup> eyes (not shown).

### *Smad7-Ad-Treated and Smad3<sup>-/-</sup> Corneas Show Reduced Expression of Growth Factors and Metalloproteases after Alkali Injury Compared to Their Controls*

Because various cytokines and matrix-degrading enzymes induced after injury are known to be regulated, in part, through the TGF- $\beta$ /Smad signaling pathway, we examined the effects of Smad7-Ad treatment and loss of Smad3 on expression of such target genes implicated in the tissue destruction in alkali-burned corneas. It is known that Smad3 signaling contributes to autoinduction of TGF- $\beta$ 1 in many

injured tissues, and that this results in elevated levels of peptide that typically persist long after the initial injury. Immunohistochemical staining showed that TGF- $\beta$ 1 and TGF- $\beta$ 2 were both expressed in the epithelium of the uninjured cornea (Figure 6A) . Although the level of expression of intracellular TGF- $\beta$ 1 in epithelium did not change substantially after injury (not shown) levels of extracellular TGF- $\beta$ 1 were significantly elevated at day 10 (not shown) and persisted at day 20 after injury in Cre-Ad-treated eyes (Figure 6A, b) . A similar pattern was observed for TGF- $\beta$ 2, with stromal expression of TGF- $\beta$ 2 being particularly intense at day 20 (Figure 6A, e) . This up-regulation of TGF- $\beta$ 1 and TGF- $\beta$ 2 was suppressed by Smad7-Ad treatment (Figure 6A, c and f) . The expression patterns of both TGF- $\beta$ 1 and TGF- $\beta$ 2 in Smad3<sup>-/-</sup> mice compared to Smad3<sup>+/+</sup> mice were similar to that seen in corneas treated by Smad7-Ad compared to Cre-Ad (data not shown).

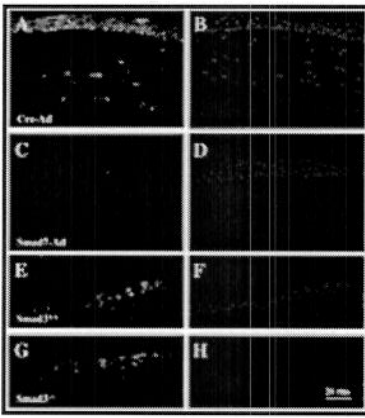


**View larger version (60K):**  
[\[in this window\]](#)  
[\[in a new window\]](#)

**Figure 6.** Expression of cytokines and growth factors in burned corneas. **A:** Immunohistochemical detection of extracellular TGF- $\beta$ 1 (**a**) and TGF- $\beta$ 2 (**b**) in representative uninjured corneas and in burned corneas treated with either Cre-Ad (**b**, **e**) or Smad7-Ad (**c**, **f**) at day 20 after injury. Accumulation of extracellular TGF- $\beta$ 1 and of TGF- $\beta$ 2 is increased in the burned stroma of the Cre-Ad group (**b**, **e**) as compared with that in Smad7-Ad group (**c**, **f**) at day 20. Nuclei are counterstained with hematoxylin. **B:** Quantitation of mRNAs of *TGF- $\beta$ 1*, *TGF- $\beta$ 2*, *MCP-1*, *MMP-9*, and *TIMP-2* by real-time RT-PCR at days 10 and 20 after injury in corneas of C57BL/6 mice treated with either Cre-Ad (red) or Smad7-Ad (pink) or in corneas of Smad3<sup>+/+</sup> (blue) or Smad3<sup>-/-</sup> mice (light blue). Real-time RT-PCR shows a marked up-regulation mRNAs of *TGF- $\beta$ 1*, *TGF- $\beta$ 2*, *MCP-1*, *MMP-9*, and *TIMP-2* in burned corneas of Cre-Ad-treated C57BL/6 mice and in those of Smad3<sup>+/+</sup> mice as compared to levels in the uninjured cornea, and this up-regulation is dramatically suppressed by Smad7 gene transfer or in corneas of mice lacking Smad3 at days 10 and 20. Data represent a typical result in one experiment of three to four done at each time point. Scale bar, 50  $\mu$ m.

MCP-1, VEGF, and CTGF were all detected immunohistochemically in epithelium and stromal cells in healing postalkali-burned corneas in the Cre-Ad group, and expression of these cytokines was markedly reduced by Smad7-Ad treatment (data not shown). Real-time RT-PCR also showed a marked up-regulation mRNAs of *TGF- $\beta$ 1*, *TGF- $\beta$ 2*, *mcp-1*, *mmp-9*, and *timp-2* in burned corneas of Cre-Ad-treated C57BL/6 mice and those of Smad3<sup>+/+</sup> mice, compared to their respective controls at days 10 and 20 (Figure 7B) .

**Figure 7.** Effect of Smad7 expression on signal transduction through the NF- $\kappa$ B pathway. In a representative cornea treated with Cre-Ad, phospho-p65/RelA is detected in the nuclei of



**View larger version (31K):**  
[\[in this window\]](#)  
[\[in a new window\]](#)

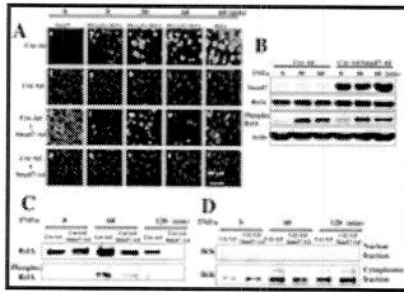
healing peripheral epithelium and stromal cells (A), whereas it can be seen only faintly in the healing central epithelium in a cornea treated with Smad7-Ad (C). In contrast, no difference is seen in peripheral corneas of Smad3<sup>+/+</sup> compared to Smad3<sup>-/-</sup> mice. B, D, F, and H represent DAPI nuclear staining corresponding to A, C, E, and G, respectively. Nuclei are counterstained with DAPI. Scale bar, 20  $\mu$ m.

### *Reduction in NF- $\kappa$ B Signaling Distinguishes Smad7-Ad-Treated Corneas from Corneas of Smad3<sup>-/-</sup> Mice after Alkali Injury*

NF- $\kappa$ B mediates signaling from many inflammatory cytokines. It was recently reported that Smad7 inhibits NF- $\kappa$ B signaling independently of its effects on Smad2/3 phosphorylation.<sup>52</sup> Indeed, evaluation of the status of NF- $\kappa$ B signaling in burned corneas showed that the phospho-p65/RelA subunit of NF- $\kappa$ B was detected in epithelial cells and stromal cells of Cre-Ad-treated corneas (Figure 7A)□, but not in corneas of the Smad7-Ad group (Figure 7C)□. Importantly, epithelial staining for phospho-p65/RelA was not reduced in Smad3<sup>-/-</sup> corneas as compared to Smad3<sup>+/+</sup> corneas, suggesting that Smad3 is not involved in the regulation of NF- $\kappa$ B signaling in this model (Figure 7, E and G)□.

To further confirm the suppressive effect of ectopic Smad7 on NF- $\kappa$ B signaling, we performed immunocytochemistry and Western blotting using an SV40-immortalized human corneal epithelial cell line (Araki-Sasaki's cell) treated with either Cre-Ad or Smad7-Ad. Immunostaining showed that exogenous Smad7 did not affect immunolocalization of RelA and phospho-RelA at 30 minutes after TNF- $\alpha$  addition (Figure 8A, c and m)□ despite strongly increased immunoreactivity for Smad7 protein (Figure 8A, a compared to k)□, but suppressed nuclear translocation of phospho-RelA and expression RelA at 60 minutes (Figure 8A; d, n, and e, o)□. In contrast, Western blotting of the total cell lysate showed that overexpression of exogenous Smad7 did not affect the levels of RelA and phospho-RelA up to 60 minutes (Figure 8B)□. Because phospho-RelA is translocated into the nucleus, we then analyzed the effect of Smad7 overexpression on its nuclear translocation. Western blotting of the nuclear fraction for RelA and phospho-RelA (Figure 8C)□ showed that nuclei of cells treated with Smad7-Ad contained substantially less RelA and phospho-RelA than those of cells treated with Cre-Ad at both 60 and 120 minutes after addition of TNF- $\alpha$ . The purity of the nuclear fractions were confirmed by the absence of staining for the cytoplasmic protein I  $\kappa$  kinase  $\alpha$  (Figure 8D)□. These results indicate that ectopic Smad7 does not alter phosphorylation of NF- $\kappa$ B/RelA in these cells, but attenuates nuclear localization of both RelA and phospho-RelA.





**View larger version (50K):**  
[\[in this window\]](#)  
[\[in a new window\]](#)

**Figure 8.** Suppression of NF- $\kappa$ B signaling by Smad7 overexpression in SV40-immortalized corneal epithelial cells. **A:** Immunocytochemistry confirms the high level of Smad7 expression in cells treated with Smad7-Ad (**k**). There is no obvious difference in expression of phospho-RelA between Cre-Ad and Smad7-Ad-treated cultures up to 30 minutes after TNF- $\alpha$  addition (**b** versus **l**, **c** versus **m**). At 60 minutes of exposure to TNF- $\alpha$ , staining for phospho-RelA (**d** versus **n**) and total RelA (**e** versus **o**) in the nuclei is reduced in the cells treated with Smad7-Ad as compared with Cre-Ad. **f** to **j** and **p** to **t**: Nuclear localization as stained with DAPI corresponding to **a** to **e** and **k** to **o**. Nuclei are counterstained with DAPI. **B:** Western blotting of total cell lysates shows that overexpression of exogenous Smad7 did not affect the level of RelA and phospho-RelA up to 60 minutes after TNF- $\alpha$  addition. **C:** Western blotting of nuclear fractions shows that total RelA, but not phospho-RelA can be detected in untreated Cre-Ad and Smad7-Ad cultures (time 0), At 60 and 120 minutes after TNF- $\alpha$  addition, Smad7-Ad suppresses TNF- $\alpha$ -induced up-regulation of nuclear translocation of total RelA and phospho-RelA. **D:** Immunodetection of I $\kappa$  kinase (IKK) in the nuclear fractions used in **C** and the corresponding cytoplasmic fractions derived from each cell culture. IKK is detected in the cytoplasmic fraction, but not in nuclear fraction, indicating the fraction is not contaminated. Scale bar, 200  $\mu$ m.

## ► Discussion

In the present study we show that adenoviral gene transfer of Smad7 prevents tissue destruction in a mouse cornea burned with a topical application of 1 N NaOH. Corneas of the control Cre-Ad group exhibited ulceration, scarring, and neovascularization, as well as conjunctivalization of the resurfaced epithelium at the final time point of day 20. In contrast, burned corneas treated with Smad7-Ad were resurfaced with a cornea-like epithelium and healed with no, or minimal, scarring as evidenced by restored transparency at day 20. Expression of exogenous Smad7 at early times after injury (up to day 5) was sufficient to improve healing as expression fell to control levels at later times, despite repeated infection at days 10 and 20. Our immunohistochemical data suggest that the mechanisms whereby overexpression of Smad7 improves healing of alkali-burned corneas involve blocking not only of Smad2/3 signaling, but possibly also of signaling leading to activation and nuclear translocation of NF- $\kappa$ B, a dimeric transcription factor activated most commonly by proinflammatory cytokines including TNF- $\alpha$  and interleukin-1.<sup>62-65</sup> At a cellular level, Smad7-Ad likely prevents corneal ulceration and stromal opacification directly by modulating Smad and/or NF- $\kappa$ B signaling in conjunctival epithelial cells, keratocytes/myofibroblasts and indirectly by reducing their expression of growth factors and cytokines/chemokines that both feedback on these two target pathways and

- ▲ Top
- ▲ Abstract
- ▲ Materials and Methods
- ▲ Results
- Discussion
- ▼ References

contribute in other ways to the outcome.

### *Effect of Smad7 on Stromal Wound Healing in the Injured Cornea*

Transient conversion of keratocytes to myofibroblasts, as characterized by expression of  $\alpha$ -SMA,<sup>58-61</sup> is one of the most important elements of corneal stromal wound healing after exposure to alkali and is associated with up-regulation of matrix components involved in stromal scarring. Although *in vitro* studies have shown that expression of  $\alpha$ -SMA in dermal fibroblasts is regulated by cytokines and extracellular matrix, ie, fibronectin ED-A<sup>54</sup>, TGF- $\beta$ /Smad2 signaling is essential for it.<sup>66-69</sup> In the present study, treatment with Smad7-Ad completely abolished expression of  $\alpha$ -SMA in keratocytes in burned stroma, whereas it was only partially reduced in corneas lacking Smad3. Although the data suggest that blocking of both Smad2 and Smad3 signaling may be necessary to completely inhibit expression of  $\alpha$ -SMA, the reduction of expression of TGF- $\beta$ 1 and of matrix proteins that modulate  $\alpha$ -SMA expression in Smad3<sup>-/-</sup> mice likely contributes indirectly to its down-regulation. These mechanisms are distinct from those implicated in myofibroblast differentiation after injury to the kidney, lens, or retina, where myofibroblasts are generated by epithelial-mesenchymal transition (EMT) of renal tubular epithelial cells, lens epithelial cells, or retinal pigment epithelial cells, respectively.<sup>36-38,44</sup> In those cases, an unidentified early step in the differentiation is completely blocked in the absence of Smad3.

Stromal scarring and opacification are believed to be dependent, in part, on up-regulation of TGF- $\beta$ 1, causing stromal cells to express extracellular matrix components qualitatively and quantitatively different from those found in uninjured stroma. Up-regulation of TGF- $\beta$ 1 in the burned cornea was completely blocked by loss of Smad3 or by treatment of injured eyes with Smad7-Ad, consistent with its dependence on Smad3. Regulation of MMP/TIMP levels, important in degradation and remodeling of stromal extracellular matrix, has been implicated in modulation of stromal opacification.<sup>6-9</sup> Expression of *mmp-9* and *timp-2* were both suppressed in corneas of Smad7-Ad-treated or Smad3<sup>-/-</sup> mice, compared to their respective controls, suggesting an altered pattern of remodeling (turnover) of matrix macromolecules in corneas in which Smad3 signaling is blocked.

Neovascularization of corneal stroma also potentially contributes to opacification. Suppression of the up-regulation of VEGF expression by treatment of alkali-burned corneas with Smad7-Ad correlates with reduced stromal neovascularization. Moreover, in corneas treated with Smad7-Ad, reduced levels of VEGF, as well as TGF- $\beta$  and MCP-1, each of which is capable of recruiting monocytes/macrophages to sites of injury likely contribute to the reduced recruitment and invasion of inflammatory cells, which themselves are capable of VEGF production. Our unpublished data showing suppression of neovascularization after alkali burn by topical administration of an adenoviral vector expressing the soluble VEGF receptor (S. Saika, K. Ikeda, O. Yamanaka, unpublished data) further support the possible role of the reduction of VEGF level in suppression of stromal neovascularization.

### *Effect of Interference with Smad Signaling on Epithelial Wound Healing in an Alkali Burned Cornea*

In the burn model we have described here, defects in the corneal epithelium resulting from alkali injury were replaced by conjunctival epithelium lacking keratin 12, similar to that seen in the clinical setting.<sup>1-3</sup> Importantly, histological analysis showed a transdifferentiation to a cornea-like epithelium in resurfaced corneas of the Smad7-Ad group and Smad3<sup>-/-</sup> mice, while the resurfaced epithelium in the Cre-Ad group and in Smad3<sup>+/+</sup> mice retained its conjunctival nature, as evidenced by the presence of goblet cells (conjunctivalization). The similar effect of overexpression of Smad7 and loss of Smad3 on the epithelial phenotype, suggest that this particular effect of Smad7 is likely dependent on its ability to block the Smad3 pathway. This difference in the phenotype of the conjunctival epithelium may also contribute to the lack of effectiveness of repeated Smad7-Ad applications at days 10 and 15, because conjunctival epithelium is more susceptible to adenoviral infection than corneal epithelium.<sup>56</sup> It was recently reported that differentiation of conjunctival epithelium resurfacing the injured corneal surface depends on the level of VEGF in the tissue.<sup>22</sup> The suppressed levels of VEGF shown here in alkali-injured corneas treated with Smad7-Ad or in Smad3<sup>-/-</sup> burned corneas, together with our demonstration that adenoviral gene transfer of soluble VEGF receptor suppressed conjunctivalization of the healing epithelium in the same type of mouse corneal alkali burn (S. Saika, K. Ikeda, O. Yamanaka, unpublished data) suggest that a reduction of VEGF might contribute to the cornea-like differentiation of resurfacing conjunctival epithelium as well as to reduced neovascularization of the injured stroma.

#### *Expression of Smad7 Blocks Not Only Smad2/3 Signaling but Also Signaling via NF- $\kappa$ B*

Direct comparisons between the adenoviral treated C57BL6 mice and the Smad3 mice are complicated both by effects of the mixed background of the latter and by the different approaches involving transient expression of ectopic genes versus genetic loss. Nonetheless, the strikingly similar effects of overexpression of Smad7 and of loss of Smad3 on epithelial phenotype, inflammation, neovascularization, and expression of various cytokine mediators of the response to injury clearly implicate the blocking of Smad3 in the mechanism of Smad7 action and suggest that deleterious effects of Smad signaling are most prominent in the early stages of the response to injury. Yet, other effects such as suppression of  $\alpha$ -SMA expression and effects on proliferation of the corneal epithelium clearly distinguish the mechanisms of action of these two signaling molecules. In this regard, we have demonstrated here for the first time that ectopic expression of Smad7 not only blocks Smad signaling, but also signaling through NF- $\kappa$ B *in vivo*, suggesting that blocking of both of these pathways contributes to accelerated corneal wound healing with reduced scarring/opacification. *In vitro* studies using an immortalized human corneal epithelial cell line confirmed that nuclear translocation of both RelA and phospho-RelA were reduced in cells treated with Smad7-Ad, similar to results previously reported in cultured renal podocytes.<sup>70</sup> Interestingly, this effect seems to be cell type-specific because no effect of Smad7 overexpression was seen on nuclear phospho-RelA in the human HaCat keratinocytes cell line (L. Lyakh, personal communication). Our finding of reduced NF- $\kappa$ B activation in corneas treated with Smad7-Ad likely contributes both to the repressed inflammation in response to alkali injury and to the suppressed expression of MMPs in cells,<sup>71,72</sup> and amplifies the effects of Smad7 on interference with Smad2/3 signaling in the burned cornea. Again, while avoiding a direct comparison, the reduced effect on healing of loss of Smad3 compared to Smad7-Ad-treated corneas is consistent with the lack of effect of loss of Smad3 on NF- $\kappa$ B signaling and with our data on the effectiveness of topical administration of

a cell permeable NF- $\kappa$ B inhibitor ligand (Upstate Biotechnology, Lake Placid, NY) on the healing of a mouse corneal alkali burn.<sup>73</sup> Whether the reduced phosphorylation of the p65/RelA subunit of NF- $\kappa$ B in corneas treated with Smad7-Ad results from direct effects of Smad7 on the pathway or indirectly from modulated expression of cytokines capable of activating the NF- $\kappa$ B pathway, cannot be determined in this model. Regardless, our data lead us to suggest that development of Smad7 delivery vectors may open new opportunities for therapeutic intervention in treatment of chemically burned corneas.

## ► Footnotes

Address reprint requests to Shizuya Saika, M.D., Ph.D., Department of Ophthalmology, Wakayama Medical University, 811-1 Kimiidera, Wakayama, 641-0012, Japan. E-mail: [shizuya@wakayama-med.ac.jp](mailto:shizuya@wakayama-med.ac.jp).

Supported by the Ministry of Education, Science, Sports, and Culture of Japan [grants C15591871 and C16590150 (to K.I.)]; the Uehara Memorial Foundation (to S.S.); the Wakayama Medical University (research grant on priority areas to S.S., Y.M., and A.O); the National Institutes of Health (grant EY 13755); Research to Prevent Blindness; and the Ohio Lions Eye Research Foundation (to W.W.-Y.K.).

Accepted for publication January 25, 2005.

## ► References

1. Brodovsky SC, McCarty CA, Snibson G, Loughnan M, Sullivan L, Daniell M, Taylor HR: Management of alkali burns: an 11-year retrospective review. *Ophthalmology* 2000, 107:1829-1835[[Medline](#)]
2. Saika S, Kobata S, Hashizume N, Okada Y, Yamanaka O: Epithelial basement membrane in alkali-burned corneas in rats. Immunohistochemical study. *Cornea* 1993, 12:383-390[[Medline](#)]
3. Ishizaki M, Zhu G, Haseba T, Shafer SS, Kao WW-Y: Expression of collagen I, smooth muscle  $\alpha$ -actin, and vimentin during the healing of alkali-burned and lacerated corneas. *Invest Ophthalmol Vis Sci* 1993, 34:3320-3328[[Abstract](#)]
4. Ravanti L, Kahari VM: Matrix metalloproteinases in wound repair. *Int J Mol Med* 2000, 6:391-407[[Medline](#)]
5. Parks WC, Wilson CL, Lopez-Boado YS: Matrix metalloproteinases as modulators of inflammation and innate immunity. *Nat Rev Immunol* 2004, 4:617-629[[Medline](#)]
6. Ye HQ, Azar DT: Expression of gelatinases A and B, and TIMPs 1 and 2 during corneal wound healing. *Invest Ophthalmol Vis Sci* 1998, 39:913-921[[Abstract](#)]
7. Kato T, Kure T, Chang JH, Gabison EE, Itoh T, Itohara S, Azar DT: Diminished corneal angiogenesis in gelatinase A-deficient mice. *FEBS Lett* 2001, 508:187-190[[Medline](#)]
8. Sivak JM, Fini ME: MMPs in the eye: emerging roles for matrix metalloproteinases in ocular physiology. *Prog Retin Eye Res* 2002, 21:1-14[[Medline](#)]
9. Daniels JT, Geerling G, Alexander RA, Murphy G, Khaw PT, Saarialho-Kere U: Temporal and spatial expression of matrix metalloproteinases during wound healing of human corneal tissue. *Exp Eye Res* 2003, 77:653-664[[Medline](#)]

<ul style="list-style-type: none"> <li>▲ <a href="#">Top</a></li> <li>▲ <a href="#">Abstract</a></li> <li>▲ <a href="#">Materials and Methods</a></li> <li>▲ <a href="#">Results</a></li> <li>▲ <a href="#">Discussion</a></li> <li>▪ <a href="#">References</a></li> </ul>
---

10. Kao WW, Liu CY, Converse RL, Shiraishi A, Kao CW, Ishizaki M, Doetschman T, Duffy J: Keratin 12-deficient mice have fragile corneal epithelia. *Invest Ophthalmol Vis Sci* 1996, 37:2572-2584[Abstract]
11. Moyer PD, Kaufman AH, Zhang Z, Kao CW, Spaulding AG, Kao WW: Conjunctival epithelial cells can resurface denuded cornea, but do not transdifferentiate to express cornea-specific keratin 12 following removal of limbal epithelium in mouse. *Differentiation* 1996, 60:31-38[Medline]
12. Sridhar MS, Bansal AK, Sangwan VS, Rao GN: Amniotic membrane transplantation in acute chemical and thermal injury. *Am J Ophthalmol* 2000, 130:134-137[Medline]
13. Meller D, Pires RT, Mack RJ, Figueiredo F, Heiligenhaus A, Park WC, Prabhawat P, John T, McLeod SD, Steuhl KP, Tseng SC: Amniotic membrane transplantation for acute chemical or thermal burns. *Ophthalmology* 2000, 107:980-989[Medline]
14. Saika S, Okada Y, Miyamoto T, Yamanaka O, Ohnishi Y, Ooshima A, Liu CY, Weng D, Kao WW: Role of p38 MAP kinase in regulation of cell migration and proliferation in healing corneal epithelium. *Invest Ophthalmol Vis Sci* 2004, 45:100-109[Abstract/Free Full Text]
15. Andresen JL, Ehlers N: Chemotaxis of human keratocytes is increased by platelet-derived growth factor-BB, epidermal growth factor, transforming growth factor-alpha, acidic fibroblast growth factor, insulin-like growth factor-I, and transforming growth factor-beta. *Curr Eye Res* 1998, 17:79-87[Medline]
16. You L, Kruse FE: Differential effect of activin A and BMP-7 on myofibroblast differentiation and the role of the Smad signaling pathway. *Invest Ophthalmol Vis Sci* 2002, 43:72-81 [Abstract/Free Full Text]
17. Ashcroft GS, Yang X, Glick AB, Weinstein M, Letterio JL, Mizel DE, Anzano M, Greenwell-Wild T, Wahl SM, Deng C, Roberts AB: Mice lacking Smad3 show accelerated wound healing and an impaired local inflammatory response. *Nat Cell Biol* 1999, 1:260-266[Medline]
18. Nakagawa T, Li JH, Garcia G, Mu W, Piek E, Bottinger EP, Chen Y, Zhu HJ, Kang DH, Schreiner GF, Lan HY, Johnson RJ: TGF- $\beta$  induces proangiogenic and antiangiogenic factors via parallel but distinct Smad pathways. *Kidney Int* 2004, 66:605-613[Medline]
19. Abraham S, Sawaya BE, Safak M, Batuman O, Khalili K, Amini S: Regulation of MCP-1 gene transcription by Smads and HIV-1 Tat in human glial cells. *Virology* 2003, 309:196-202[Medline]
20. Edelman JL, Castro MR, Wen Y: Correlation of VEGF expression by leukocytes with the growth and regression of blood vessels in the rat cornea. *Invest Ophthalmol Vis Sci* 1999, 40:1112-1123 [Abstract]
21. Lai CM, Spilsbury K, Brankov M, Zaknich T, Rakoczy PE: Inhibition of corneal neovascularization by recombinant adenovirus mediated antisense VEGF RNA. *Exp Eye Res* 2002, 75:625-634[Medline]
22. Jousen AM, Poulaki V, Mitsiades N, Stechschulte SU, Kirchhof B, Dartt DA, Fong GH, Rudge J, Wiegand SJ, Yancopoulos GD, Adamis AP: VEGF-dependent conjunctivalization of the corneal surface. *Invest Ophthalmol Vis Sci* 2003, 44:117-123[Abstract/Free Full Text]
23. Barleon B, Sozzani S, Zhou D, Weich HA, Mantovani A, Marme D: Migration of human monocytes in response to vascular endothelial growth factor (VEGF) is mediated via the VEGF receptor flt-1. *Blood* 1996, 87:3336-3343[Abstract/Free Full Text]
24. Yang ZF, Poon RT, Luo Y, Cheung CK, Ho DW, Lo CM, Fan ST: Up-regulation of vascular endothelial growth factor (VEGF) in small-for-size liver grafts enhances macrophage activities through VEGF receptor 2-dependent pathway. *J Immunol* 2004, 173:2507-2515 [Abstract/Free Full Text]
25. Tesch GH, Schwarting A, Kinoshita K, Lan HY, Rollins BJ, Kelley VR: Monocyte chemoattractant protein-1 promotes macrophage-mediated tubular injury, but not glomerular injury, in nephrotoxic serum nephritis. *J Clin Invest* 1999, 103:73-80[Abstract/Free Full Text]
26. Low QE, Drugea IA, Duffner LA, Quinn DG, Cook DN, Rollins BJ, Kovacs EJ, DiPietro LA: Wound healing in MIP-1 $\alpha$ (-/-) and MCP-1(-/-) mice. *Am J Pathol* 2001, 159:457-463 [Abstract/Free Full Text]

27. Pfister RR, Haddox JL, Sommers CI: Injection of chemoattractants into normal cornea: a model of inflammation after alkali injury. *Invest Ophthalmol Vis Sci* 1998, 39:1744-1750[[Abstract](#)]
28. Massague J, Wotton D: Transcriptional control by the TGF- $\beta$ /Smad signaling system. *EMBO J* 2000, 19:1745-1754[[Abstract/Free Full Text](#)]
29. Moustakas A, Pardali K, Gaal A, Heldin CH: Mechanisms of TGF- $\beta$  signaling in regulation of cell growth and differentiation. *Immunol Lett* 2002, 82:85-91[[Medline](#)]
30. ten Dijke P, Goumans MJ, Itoh F, Itoh S: Regulation of cell proliferation by Smad proteins. *J Cell Physiol* 2002, 191:1-16[[Medline](#)]
31. Derynck R, Zhang YE: Smad-dependent and Smad-independent pathways in TGF- $\beta$  family signalling. *Nature* 2003, 425:577-584[[Medline](#)]
32. Roberts AB, Piek E, Bottinger EP, Ashcroft G, Mitchell JB, Flanders KC: Is Smad3 a major player in signal transduction pathways leading to fibrogenesis? *Chest* 2001, 120(Suppl 1):43S-47S
33. Schnabl B, Kweon YO, Frederick JP, Wang XF, Rippe RA, Brenner DA: The role of Smad3 in mediating mouse hepatic stellate cell activation. *Hepatology* 2001, 3:89-100
34. Flanders KC, Sullivan CD, Fujii M, Sowers A, Anzano MA, Arabshahi A, Major C, Deng C, Russo A, Mitchell JB, Roberts AB: Mice lacking Smad3 are protected against cutaneous injury induced by ionizing radiation. *Am J Pathol* 2002, 160:1057-1068[[Abstract/Free Full Text](#)]
35. Sato M, Muragaki Y, Saika S, Roberts AB, Ooshima A: Targeted disruption of TGF- $\beta$ 1/Smad3 signaling protects against renal tubulointerstitial fibrosis induced by unilateral ureteral obstruction. *J Clin Invest* 2003, 112:1486-1494[[Abstract/Free Full Text](#)]
36. Flanders KC, Major CD, Arabshahi A, Aburime EE, Okada MH, Fujii M, Blalock TD, Schultz GS, Sowers A, Anzano MA, Mitchell JB, Russo A, Roberts AB: Interference with transforming growth factor- $\beta$ / Smad3 signaling results in accelerated healing of wounds in previously irradiated skin. *Am J Pathol* 2003, 163:2247-2257[[Abstract/Free Full Text](#)]
37. Saika S, Kono-Saika S, Ohnishi Y, Sato M, Muragaki Y, Ooshima A, Flanders KC, Yoo J, Anzano M, Liu CY, Kao WW, Roberts AB: Smad3 signaling is required for epithelial-mesenchymal transition of lens epithelium after injury. *Am J Pathol* 2004, 164:651-663 [[Abstract/Free Full Text](#)]
38. Flanders KC: Smad3 as a mediator of the fibrotic response. *Int J Exp Pathol* 2004, 85:47-64 [[Medline](#)]
39. Bonniaud P, Kolb M, Galt T, Robertson J, Robbins C, Stampfli M, Lavery C, Margetts PJ, Roberts AB, Gauldie J: Smad3 null mice develop airspace enlargement and are resistant to TGF- $\beta$ -mediated pulmonary fibrosis. *J Immunol* 2004, 173:2099-2108[[Abstract/Free Full Text](#)]
40. Saika S, Kono-Saika S, Tanaka T, Yamanaka O, Ohnishi Y, Sato M, Muragaki Y, Ooshima A, Yoo J, Flanders KC, Roberts AB: Smad3 is required for dedifferentiation of retinal pigment epithelium following retinal detachment in mice. *Lab Invest* 2004, 84:1245-1258[[Medline](#)]
41. Hayashi H, Abdollah S, Qiu Y, Cai J, Xu YY, Grinnell BW, Richardson MA, Topper JN, Gimbrone MA, Jr, Wrana JL, Falb D: The MAD-related protein Smad7 associates with the TGF $\beta$  receptor and functions as an antagonist of TGF $\beta$  signaling. *Cell* 1997, 89:1165-1173[[Medline](#)]
42. Nakao A, Afrakhte M, Moren A, Nakayama T, Christian JL, Heuchel R, Itoh S, Kawabata M, Heldin NE, Heldin CH, ten Dijke P: Identification of Smad7, a TGF $\beta$ -inducible antagonist of TGF- $\beta$  signalling. *Nature* 1997, 389:631-635[[Medline](#)]
43. Pulaski L, Landstrom M, Heldin CH, Souchelnytskyi S: Phosphorylation of Smad7 at Ser-249 does not interfere with its inhibitory role in transforming growth factor-beta-dependent signaling but affects Smad7-dependent transcriptional activation. *J Biol Chem* 2001, 276:14344-14349 [[Abstract/Free Full Text](#)]
44. Nakao A, Fujii M, Matsumura R, Kumano K, Saito Y, Miyazono K, Iwamoto I: Transient gene transfer and expression of Smad7 prevents bleomycin-induced lung fibrosis in mice. *J Clin Invest* 1999, 104:5-11[[Abstract/Free Full Text](#)]
45. Lan HY, Mu W, Tomita N, Huang XR, Li JH, Zhu HJ, Morishita R, Johnson RJ: Inhibition of renal fibrosis by gene transfer of inducible Smad7 using ultrasound-microbubble system in rat

- UUO model. *J Am Soc Nephrol* 2003, 14:1535-1548[[Abstract/Free Full Text](#)]
46. Dooley S, Hamzavi J, Breitkopf K, Wiercinska E, Said HM, Lorenzen J, Ten Dijke P, Gressner AM: Smad7 prevents activation of hepatic stellate cells and liver fibrosis in rats. *Gastroenterology* 2003, 125:178-191[[Medline](#)]
  47. Saika S, Ikeda K, Yamanaka O, Sato M, Muragaki Y, Ohnishi Y, Ooshima A, Nakajima Y, Namikawa K, Kiyama H, Flanders KC, Roberts AB: Transient adenoviral gene transfer of Smad7 prevents injury-induced epithelial-mesenchymal transition of lens epithelium in mice. *Lab Invest* 2004, 84:1259-1270[[Medline](#)]
  48. Bitzer M, von Gersdorff G, Liang D, Dominguez-Rosales A, Beg AA, Rojkind M, Bottinger EP: A mechanism of suppression of TGF- $\beta$ /SMAD signaling by NF- $\kappa$ B/RelA. *Genes Dev* 2000, 14:187-197[[Abstract/Free Full Text](#)]
  49. Lopez-Rovira T, Chalaux E, Rosa JL, Bartrons R, Ventura F: Interaction and functional cooperation of NF-kappa B with Smads. Transcriptional regulation of the junB promoter. *J Biol Chem* 2000, 275:28937-28946[[Abstract/Free Full Text](#)]
  50. Monteleone G, Mann J, Monteleone I, Vavassori P, Bremner R, Fantini M, Del Vecchio Blanco G, Tersigni R, Alessandrini L, Mann D, Pallone F, MacDonald TT: A failure of transforming growth factor-beta1 negative regulation maintains sustained NF- $\kappa$ B activation in gut inflammation. *J Biol Chem* 2004, 279:3925-3932[[Abstract/Free Full Text](#)]
  51. Lallemand F, Mazars A, Prunier C, Bertrand F, Kornprost M, Gallea S, Roman-Roman S, Cherqui G, Atfi A: Smad7 inhibits the survival nuclear factor kappaB and potentiates apoptosis in epithelial cells. *Oncogene* 2001, 20:879-884[[Medline](#)]
  52. Saika S, Shiraishi A, Liu CY, Funderburgh JL, Kao CW, Converse RL, Kao WW: Role of lumican in the corneal epithelium during wound healing. *J Biol Chem* 2000, 275:2607-2612 [[Abstract/Free Full Text](#)]
  53. Saika S, Saika S, Liu CY, Azhar M, Sanford LP, Doetschman T, Gendron RL, Kao CW, Kao WW: TGF $\beta$ 2 in corneal morphogenesis during mouse embryonic development. *Dev Biol* 2001, 240:419-432[[Medline](#)]
  54. Flanders KC, Thompson NL, Cissel DS, Van Obberghen-Schilling E, Baker CC, Kass ME, Ellingsworth LR, Roberts AB, Sporn MB: Transforming growth factor- $\beta$ 1: histochemical localization with antibodies to different epitopes. *J Cell Biol* 1989, 108:653-660[[Abstract](#)]
  55. Flanders KC, Ludecke G, Engels S, Cissel DS, Roberts AB, Kondaiah P, Lafyatis R, Sporn MB, Unsicker K: Localization and actions of transforming growth factor- $\beta$ s in the embryonic nervous system. *Development* 1991, 113:183-191[[Abstract](#)]
  56. Araki-Sasaki K, Ohashi Y, Sasabe T, Hayashi K, Watanabe H, Tano Y, Handa H: An SV40-immortalized human corneal epithelial cell line and its characterization. *Invest Ophthalmol Vis Sci* 1995, 36:614-621[[Abstract](#)]
  57. Tsubota K, Inoue H, Ando K, Ono M, Yoshino K, Saito I: Adenovirus-mediated gene transfer to the ocular surface epithelium. *Exp Eye Res* 1998, 67:531-538[[Medline](#)]
  58. Serini G, Bochaton-Piallat ML, Ropraz P, Geinoz A, Borsi L, Zardi L, Gabbiani G: The fibronectin domain ED-A is crucial for myofibroblastic phenotype induction by transforming growth factor-beta1. *J Cell Biol* 1998, 142:873-881[[Abstract/Free Full Text](#)]
  59. Tomasek JJ, Gabbiani G, Hinz B, Chaponnier C, Brown RA: Myofibroblasts and mechano-regulation of connective tissue remodelling. *Nat Rev Mol Cell Biol* 2002, 3:349-363[[Medline](#)]
  60. Jester JV, Huang J, Petroll WM, Cavanagh HD: TGF $\beta$  induced myofibroblast differentiation of rabbit keratocytes requires synergistic TGF $\beta$ , PDGF and integrin signaling. *Exp Eye Res* 2002, 75:645-657[[Medline](#)]
  61. Desmouliere A, Darby IA, Gabbiani G: Normal and pathologic soft tissue remodeling: role of the myofibroblast, with special emphasis on liver and kidney fibrosis. *Lab Invest* 2003, 83:1689-1707 [[Medline](#)]
  62. Baldwin AS, Jr: Series introduction: the transcription factor NF- $\kappa$ B and human disease. *J Clin Invest* 2001, 107:3-6[[Free Full Text](#)]

63. Tak PP, Firestein GS: NF- $\kappa$ B: a key role in inflammatory diseases. *J Clin Invest* 2001, 107:7-11 [[Free Full Text](#)]
64. Yamamoto Y, Gaynor RB: Therapeutic potential of inhibition of the NF- $\kappa$ B pathway in the treatment of inflammation and cancer. *J Clin Invest* 2001, 107:135-142 [[Free Full Text](#)]
65. Hanada T, Yoshimura A: Regulation of cytokine signaling and inflammation. *Cytokine Growth Factor Rev* 2002, 13:413-421 [[Medline](#)]
66. Piek E, Ju WJ, Heyer J, Escalante-Alcalde D, Stewart CL, Weinstein M, Deng C, Kucherlapati R, Bottinger EP, Roberts AB: Functional characterization of transforming growth factor  $\beta$  signaling in Smad2- and Smad3-deficient fibroblasts. *J Biol Chem* 2001, 276:19945-19953 [[Abstract/Free Full Text](#)]
67. Itoh S, Thorikay M, Kowanetz M, Moustakas A, Itoh F, Heldin CH, ten Dijke P: Elucidation of Smad requirement in transforming growth factor- $\beta$  type I receptor-induced responses. *J Biol Chem* 2003, 278:3751-3761 [[Abstract/Free Full Text](#)]
68. Yang YC, Piek E, Zavadil J, Liang D, Xie D, Heyer J, Pavlidis P, Kucherlapati R, Roberts AB, Bottinger EP: Hierarchical model of gene regulation by transforming growth factor  $\beta$ . *Proc Natl Acad Sci USA* 2003, 100:10269-10274 [[Abstract/Free Full Text](#)]
69. Evans RA, Tian YC, Steadman R, Phillips AO: TGF- $\beta$ 1-mediated fibroblast-myofibroblast terminal differentiation—the role of Smad proteins. *Exp Cell Res* 2003, 282:90-100 [[Medline](#)]
70. Schiffer M, Bitzer M, Roberts ISD, Kopp JB, ten Dijke P, Mundel P, Böttinger EP: Apoptosis in podocytes induced by TGF- $\beta$  and Smad7. *J Clin Invest* 2001, 108:807-816 [[Abstract/Free Full Text](#)]
71. Bond M, Fabunmi RP, Baker AH, Newby AC: Synergistic upregulation of metalloproteinase-9 by growth factors and inflammatory cytokines: an absolute requirement for transcription factor NF- $\kappa$ B. *FEBS Lett* 1998, 435:29-34 [[Medline](#)]
72. Bond M, Baker AH, Newby AC: Nuclear factor  $\kappa$ B activity is essential for matrix metalloproteinase-1 and -3 upregulation in rabbit dermal fibroblasts. *Biochem Biophys Res Commun* 1999, 264:561-567 [[Medline](#)]
73. Saika S, Miyamoto T, Yamanaka O, Kato T, Ohnishi Y, Flanders KC, Ikeda K, Nakajima Y, Kao WW-Y, Sdato M, Muragaki Y, Ooshima A: Therapeutic effect of topical administration of SN50, an inhibitor of NF- $\kappa$ B, in treatment of corneal alkali burns in mice. *Am J Pathol* 2005, 166:1393-1403 [[Abstract/Free Full Text](#)]

**This article has been cited by other articles:** ([Search Google Scholar for Other Citing Articles](#))



The American Journal of **PATHOLOGY**

[HOME](#)

S. Saika, K. Ikeda, O. Yamanaka, K. C. Flanders, Y. Okada, T. Miyamoto, A. Kitano, A. Ooshima, Y. Nakajima, Y. Ohnishi, and W. W.-Y. Kao

**Loss of Tumor Necrosis Factor {alpha} Potentiates Transforming Growth Factor {beta}-mediated Pathogenic Tissue Response during Wound Healing**

*Am. J. Pathol.*, June 1, 2006; 168(6): 1848 - 1860.

[[Abstract](#)] [[Full Text](#)] [[PDF](#)]

Am. J. Physiol: Cell Physiology

[HOME](#)

S. Saika, K. Ikeda, O. Yamanaka, K. C. Flanders, Y. Ohnishi, Y. Nakajima,





Y. Muragaki, and A. Ooshima

**Adenoviral gene transfer of BMP-7, Id2, or Id3 suppresses injury-induced epithelial-to-mesenchymal transition of lens epithelium in mice**

Am J Physiol Cell Physiol, January 1, 2006; 290(1): C282 - C289.

[\[Abstract\]](#) [\[Full Text\]](#) [\[PDF\]](#)



The American Journal of **PATHOLOGY**

[▶ HOME](#)

S. Saika, T. Miyamoto, O. Yamanaka, T. Kato, Y. Ohnishi, K. C. Flanders, K. Ikeda, Y. Nakajima, W. W.-Y. Kao, M. Sato, Y. Muragaki, and A. Ooshima

**Therapeutic Effect of Topical Administration of SN50, an Inhibitor of Nuclear Factor- $\kappa$ B, in Treatment of Corneal Alkali Burns in Mice**

Am. J. Pathol., May 1, 2005; 166(5): 1393 - 1403.

[\[Abstract\]](#) [\[Full Text\]](#) [\[PDF\]](#)

*This Article*

- ▶ [Abstract](#) **FREE**
- ▶ [Full Text \(PDF\)](#)
- ▶ [Purchase Article](#)
- ▶ [View Shopping Cart](#)

*Services*

- ▶ [Similar articles in this journal](#)
- ▶ [Similar articles in PubMed](#)
- ▶ [Alert me to new issues of the journal](#)
- ▶ [Download to citation manager](#)

*Google Scholar*

- ▶ [Articles by Saika, S.](#)
- ▶ [Articles by Roberts, A. B.](#)
- ▶ [Articles citing this Article](#)

*PubMed*

- ▶ [PubMed Citation](#)
- ▶ [Articles by Saika, S.](#)
- ▶ [Articles by Roberts, A. B.](#)

[HOME](#) [HELP](#) [FEEDBACK](#) [SUBSCRIPTIONS](#) [ARCHIVE](#) [SEARCH](#) [TABLE OF CONTENTS](#)